Journal of Materials Chemistry A

Accepted Manuscript

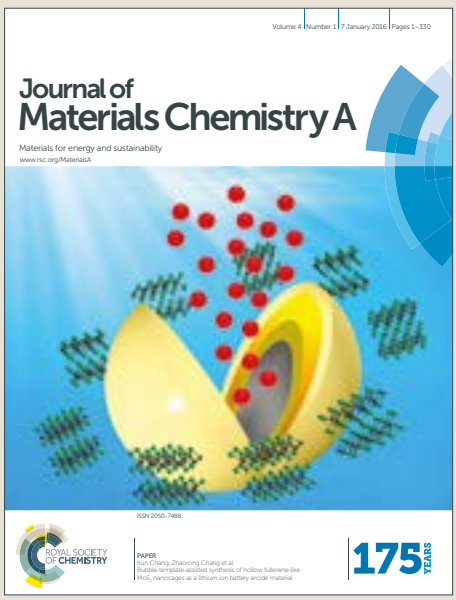

ROYAL SOCIETY OF CHEMISTRY

rsc.li/materials-a

View Article Online
DOI: 10.1039/C9TA00287A

Characterization of adsorption site energies and heterogeneous surfaces of porous materials

K. Vasanth Kumar,[1,2]* Gadipelli Srinivas,[3] Barbara Wood,[4] Kiran A Ramisetty,[2] Andrew A. Stewart,[5] Christopher A. Howard, [6] Dan Brett [3] and F. Rodriguez-Reinoso[7]

(1) Queen Mary, University of London, Mile End Road, London, E1 4NS, United Kingdom.
(2) Synthesis and Solid State Pharmaceutical Centre, Bernal Institute, University of Limerick, Limerick, Ireland.
(3) Electrochemical Innovation Lab, Department of Chemical Engineering, UCL, London, United Kingdom.
(4) Synthesis and Solid State Pharmaceutical Centre, UCD Crystallization Research Group, School of Chemical and Bioprocess Engineering, University College Dublin, Belfield, Dublin, Ireland.
(5) Department of Physics and the Bernal Institute, University of Limerick, Limerick, Ireland.
(6) Department of Physics & Astronomy, University College London, London WC1E 6BT, United Kingdom.
(7) Laboratorio de Materiales Avanzados, Departamento de Química Inorgánica-Universidad de Alicante, Ctra. San Vicente, s/n-03690 San Vicente del Raspeig. Spain.

Abstract

Characterization of the guest-host interactions and the heterogeneity of porous materials is essential across the physical and biological sciences, for example for gas sorption and separation, pollutant removal from wastewater, biological systems (protein-ligand binding) and, molecular recognition materials such as molecularly imprinted polymers. Information about the guest-host interactions can be obtained from calorimetric experiments. Alternatively, more detailed information can be obtained by properly interrogating the experimentally acquired adsorption equilibrium data. Adsorption equilibrium is usually interpreted using the theoretical adsorption isotherms that correlate the equilibrium concentration of the adsorbate in the solid phase and in the bulk fluid at a constant temperature. Such theoretical isotherms or expressions can accurately predict the adsorbent efficiency (at equilibrium) as a function of process variables such as initial adsorbate concentration, adsorbent mass, reactor volume and temperature. Detailed analysis of the adsorption isotherms permits the calculation of the number density of the adsorbent sites, their binding energy for the guest molecules and information about the distribution of adsorption site binding energies. These analyses are discussed in this review. A critical evaluation of the analytical and numerical methods that can characterize the heterogeneity; guest-host interactions involved in terms of discrete or continuous binding site affinity distribution was performed. Critical discussion of the limitations and the advantages of these models is provided. An overview of the experimental techniques that rely on calorimetric and chromatographic principles to experimentally measure the binding energy and characteristic properties of the adsorbent surfaces is also included. Finally, the potential use of the site energy distribution functions and their potential to bring new information about the adsorbents binding energy for a specific guest molecule application is discussed.

View Article Online
DOI: 10.1039/C9TA00287A

1. Introduction

Adsorption of soluble species and small molecules of gas or liquid is considered to be an important and useful technique by chemists, biologists, engineers, industrialists, environmentalists, climatologists and material scientists.[1,2] Adsorption based technologies exploit the ability of certain solids to selectively concentrate specific molecules in large quantities from solution or any bulk fluid.[3] The most commonly encountered examples include dehumidification and separation of N_2/O_2 from the air, capture of CO_2, NOx, SOx, or other toxic pollutants, and removal of volatile organic compounds, gas sensing, recovery of solvent vapours from dilute mixtures, as well as protein interactions with small molecules.[4–8] Other applications of adsorption include heterogeneous catalysis, waste water treatment, removal of objectionable odor and taste; metal leaching, storage of logistically important gases like hydrogen and methane, molecular separations and molecular gas sensosrs.[9–21] In biological systems, adsorption equilibrium characterizes the ligand-binding systems.[22] Another important application of adsorption is the removal of pollutants from an unmanageable, large volume of liquid to a manageable solid phase using low cost adsorbents which are safely disposed of after the process.[18]

The entire adsorption process can be captured by modeling the number of adsorption sites in the solid adsorbent, their type, and their binding energies for a specific adsorptive or target molecule.[23] Depending on the type of site and their binding energy, the adsorption sites emphasize themselves to uptake adsorbate molecules at different concentrations or pressures. For instance, heterogeneous adsorbents are characterized by the presence of different types of binding sites with different binding energies. Binding site heterogeneity is a commonly expected characteristic property of engineered material like activated carbon, functionalized or templated carbons. Binding site heterogeneity exists in most of the adsorbents for a number of reasons. For instance, the type of carbon precursor, the amount of activator and the pyrolysis temperature can all introduce binding site heterogeneity on the carbon surface. In some cases, site heterogeneity can arise, due to the presence of impurities on the adsorbent surface. A carbon material that is obtained from physical or steam activation usually contains a large number of oxygen atoms on the carbon surfaces in the form of hydroxyl or carboxylic groups.[24] High temperature treatment, a commonly used strategy performed while synthesizing activated carbons, usually creates defects/vacancies and pore surface curvature. The presence of heteroatoms, vacancies, functional groups as well as the pore size heterogeneity can result in different levels of binding energy for a specified target molecule. In the case of crystalline materials, the heterogeneity can arise due to atom vacancy (point defect) or line and planar defects. Any of these factors can introduce a certain level of binding site heterogeneity. In naturally occurring materials that are commonly classified as low-cost adsorbents, binding site heterogeneity can exist due to the heterogeneous nature of the material itself. For instance, in fly ash, a commonly used low cost material, such heterogeneity can arise from the natural composition of the material itself. [24]

View Article Online
DOI: 10.1039/C9TA00287A

Figure 1 shows a model of a carbon pore surface and the presence of different types of adsorption sites that introduce binding site heterogeneity. Figure 1 illustrates the complexities involved in characterizing the binding site heterogeneity of a material like activated carbon, which contains numerous amounts of functionalities and heteroatoms. It is clearly a prohibitively difficult task to probe through multiple adsorption experiments in order to exactly ascertain the type of adsorption sites (for example, there are at least six sites on the material shown in Figure 1(a)) each of which could optimally host a target molecule at a different particular pressure or concentration during the course of adsorption at equilibrium conditions.

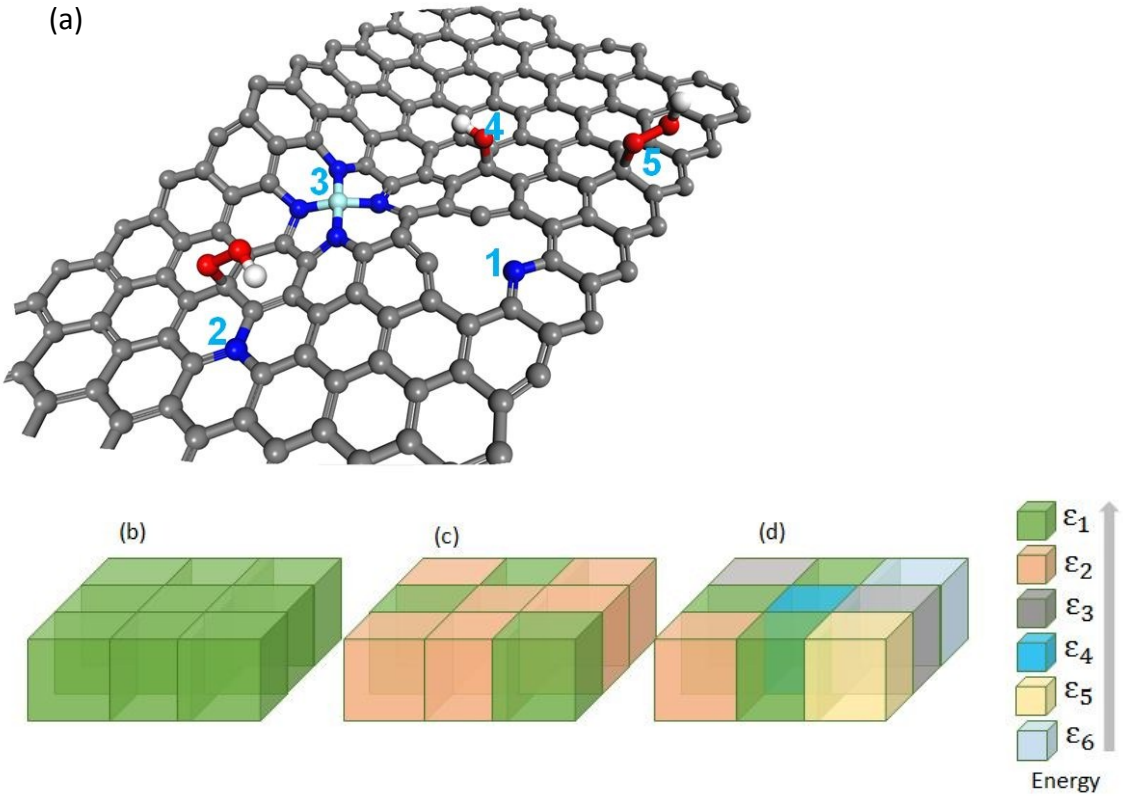

Figure 1(a): shows a possible surface that can be realized in a Fe (iron) & N (nitrogen) doped porous carbon surface prepared via chemical/physical activation methods. It is possible to expect different types of adsorption sites: (1) pyridinic N, (2) graphitic N, (3) Fe-N coordination, (4) hydroxyl group, and (5) carboxylic group. These sites possess a different level of binding energy for a specific target molecule. Apart from this, the surface curvature itself can introduce a certain level of heterogeneity. Typically, a target molecule will experience stronger binding energy on a curved surface than on a flat carbon surface since the adsorbing molecule will experience interactions from an increased number of adjacent carbon atoms. Apart from this, pore-size and its distribution will introduce more heterogeneity. Figure 1 (b-d): shows the two-dimensional adsorption surfaces that contain (b) only one type of adsorption site, (c) two types of adsorption sites and (d) six different types of adsorption sites. Figure 1(d) can be taken as a two-dimensional

View Article Online
DOI: 10.1039/C9TA00287A

representation of the adsorption site heterogeneity observed in the structure shown in Figure 1(a).

However, it is possible to get approximate information about the types of adsorption available on such a complex surface. One approach is to assume that all the adsorption sites are spread over a two-dimensional surface as shown in Figure 1(b-d), where the objective is to find how many different types of adsorption sites are available on the surface, and their binding energy. Figures 1(b) to 1(d) show three different cases of a simple two dimensional surface that contains: (Case 1) only one type of adsorption site (also shown is the associated adsorption energy), (Case 2) two different types of adsorption sites associated with adsorption energies of ε_1 and ε_2, and (Case 3) six different types of adsorption sites (their adsorption energies range from ε_1 to ε_6). For case 1, the adsorption energy required to bring a molecule from a bulk state to an adsorbed state will be roughly equivalent to ε_1. In Case 2, the simplest heterogeneous surface, containing only two different types of binding sites, can be associated with adsorption energies, ε_1 and ε_2. Both of these cases can be easily modeled using the simple theoretical adsorption isotherm. The most widely used isotherm is the Langmuir and bi-Langmuir isotherm (this is discussed in detail in later sections). Most of the porous materials used in adsorption processes contain more than two types of adsorption sites (Figure 1(d)). Figure 1(d) shows a model two-dimensional surface that contains six different types of binding sites which are associated with different levels of adsorption energies that range from ε_1 to ε_6 (where, $\varepsilon_1>\varepsilon_2>\varepsilon_3>\varepsilon_4>\varepsilon_5>\varepsilon_6$). Determining the adsorption energy and obtaining information about the site energy distribution (such as whether they are uniformly distributed or exponentially distributed), the mean adsorption site energy, the number of adsorption sites and their types directly from the adsorption equilibrium data or using simple theoretical adsorption isotherm like a Langmuir isotherm is not a trivial task.

Though an accurate prediction of the adsorption site energy distribution is difficult, adsorption theories can allow us to estimate the number of binding sites available on the surface for a specific target molecule. With some theoretical approximations, it is also possible to estimate how many types of adsorption sites are available on the surface and their associated binding energies. At a fixed temperature, T, the adsorption site with the highest binding energy can adsorb the target molecule from the bulk phase in very low concentrations. Likewise, the adsorption sites with the weakest binding energy for a specific target molecule, can adsorb the pollutant only if the concentration of the adsorbate in the liquid phase is relatively higher or at higher pressures during the adsorption of gas molecules. By properly exploiting these particular adsorption phenomena, the characteristic surface properties of an adsorbent (in terms of the adsorption site energy distribution) can be quantified experimentally by measuring the number of solute molecules adsorbed over a wide range of equilibrium concentrations or pressures. With recent advancements in instrumentation and analytical techniques, it is now easier to obtain high quality adsorption isotherms over a wide range of equilibrium pressures and concentrations. Additionally, unless the solubility of the target molecule exceeds the number of binding sites on the adsorbent surface, it is always possible to titrate all the available binding sites with the target molecules at equilibrium conditions.

View Article Online
DOI: 10.1039/C9TA00287A

To date, adsorption equilibrium data obtained at cryogenic conditions has been widely used to characterize the material properties (for small molecules) in terms of surface area and pore characteristics. These pore characteristics include pore-size, pore-size distribution and pore-volume.[25] Alternatively, the equilibrium gas adsorption data obtained at cryogenic temperatures (or at any temperature from either the gas or liquid phase) can provide information about the surface heterogeneity of the solid material. This can be achieved by using a mathematical function commonly referred to as the affinity distribution function (ADF) though it can be referred to as the adsorption site energy distribution function.[26–29] The concept of estimating the ADFs relies on a simple model; an adsorbent surface contains numerous adsorption sites, each with a different level of binding energy for the target molecule. According to the adsorption theory, these adsorption sites with different levels of binding energies for a specific target molecule can uptake that adsorptive molecule and remain in equilibrium with the bulk fluid, depending on the concentration of the solution (in the case of liquid adsorption) or the pressure of the bulk fluid (in the case of gas adsorption). The ADFs can be either discrete or continuous and usually the spectra or the points generated by these functions are called binding (or adsorption) site energy distribution spectra or binding affinity spectra.[30,31] In most cases these mathematical functions rely on either a theoretical adsorption isotherm or on the experimental equilibrium data and do not require any additional sophisticated instrumentation. Alternatively, the ADF can reveal the energetic sites that are already occupied or the energetic sites that are available to host a guest molecule as a function of pressure or concentration. ADFs can even be used to bring theoretical meaning to the empirical expressions that are commonly used to model adsorption equilibrium data.

In this review, a detailed and critical analysis is presented on the available mathematical functions, empirical approaches, different mathematical models and few numerical techniques that allow us to exploit to the core the experimental equilibrium data or a theoretical adsorption isotherm. These analyses permit characterization of the energetic heterogeneities of the adsorbent surface and to provide detailed information about the guest-host interactions. The main advantages of these methods are discussed and some of the limitations of these approaches are highlighted in selected sections. The frequently used theoretical adsorption isotherms and how they can complement the ADFs in revealing the binding site heterogeneity of the adsorbents is discussed. Also demonstrated is how these distribution functions can be used to propose a theoretical background for an empirical adsorption isotherm such as Freundlich or Redlich-Peterson isotherms.[32,33] The central purpose of this review is to highlight the advantages of these mathematical functions and how they can push the use of theoretical adsorption isotherms such as Freundlich, Langmuir, Redlich-Peterson, Freundlich-Langmuir (or any other isotherm)to the next level, for example, for the characterization of an adsorbent surface by estimating the number and the type of adsorption sites and their binding energies and how they are distributed within the adsorbent. A separate section is dedicated to the isosteric heat of adsorption, which is a powerful method to characterize the binding site heterogeneity or to quantify the guest-host interaction energies. To complement the ADFs, the advantages and the limitations of several experimental techniques including frontal affinity chromatography and immersion calorimetry

View Article Online
DOI: 10.1039/C9TA00287A

are also discussed. These techniques either directly or indirectly provide information similar to that obtained from ADFs. Through experimental titration, the binding sites available on the adsorbent surface can be obtained along with characteristic and reliable information about the binding site heterogeneity.

This review is presented in 14 sections. Following this introduction section, the concept of binding energy and the basic theory is defined in Section 2. In Section 3, the use of adsorption isotherms to rapidly obtain preliminary information about the heterogeneity of the adsorbent and the binding energy of all the sites, using a discrete site energy distribution function, is demonstrated. In Section 4 the different types of adsorbent surfaces in commonly used porous materials and the associated pictorial representations are listed. In Section 5 the limitations of discrete site energy distribution models are discussed. In Section 6, the continuous distribution function is defined and its use in characterizing the site energy distribution is demonstrated. Methods for bypassing the limitations of the discrete site energy distribution are also presented in this section. Section 7 deals with the method of Stieltjes transforms[34,35] to obtain site energy distribution functions from theoretical adsorption isotherms. In this section, the theoretical concepts of the most widely used Sips and Freundlich isotherms are also discussed. This section emphasizes the utilization of the method of Stieltjes transform to determine the distribution of adsorption site energies according to these two widely used adsorption isotherms. In Section 8, a critical analysis of the finite difference method developed originally by Hunston *et al* to obtain the continuous affinity site energy distribution is presented. In this section, the advantage of this method in terms of its simplicity in predicting the site energy distribution spectra is shown. The use of this simple technique to assist in identifying the physical background of any theoretical adsorption isotherm such as Redlich-Peterson, Sips isotherms is presented along with the way in which this technique can help to trace the change in site energy distribution spectra as a function of the adsorption isotherm parameters. In Section 9, the expectation-maximization technique, one of the most widely used methods to obtain the site energy distribution spectra in the area of adsorption chromatography, is summarized. In Section 10, the common limitations of all the techniques detailed in the earlier sections are summarized. In this section, some of the main challenges that remain in characterization of special adsorbents like flexible porous structures are highlighted. Section 11 details the principles of the isosteric heat of adsorption and the fundamentals of adsorption thermodynamics. Also described are the theoretical methods used to obtain this parameter and the way in which it can provide information about solute-solvent and solvent-solvent interactions. At the end of this section, a commentary is presented on the utilization of this parameter to complement the spectra obtained using the site energy distribution functions. In Section 12 and 13, the principles behind two experimental techniques: immersion calorimetry and frontal affinity chromatography, are briefly discussed. This section details the way in which immersion calorimetry can experimentally determine the site energy distribution. Also highlighted is the versatility of the frontal affinity chromatography technique to simultaneously obtain adsorption isotherms and measure the competition effects which usually occur during the multi-component adsorption. Additionally, the way in which both of these techniques can complement the affinity distribution spectra obtained using any of the theoretical or numerical techniques reviewed here, is presented. Finally, Section 14 provides the final remarks on the

View Article Online
DOI: 10.1039/C9TA00287A

potential applications of the affinity distribution spectra. This section identifies new specific areas in the world of materials chemistry where the site energy distribution spectra can be used as a potential theoretical tool to bring new and interesting physical insights. Some of the common limitations of the different theoretical methods that allow determining the site energy distribution spectra are also highlighted.

2. The concept of binding energy and the basic theory

Binding energy can be defined as the energy associated with the adsorption of a specific target molecule onto a specific type of adsorption site located on an adsorbent surface (site A in Figure 2(a)) within an adsorbent pore volume (site B in Figure 2(a)). A homogeneous adsorbent surface in terms of binding energy is usually assumed to contain only one type of adsorption site. Imagine a hypothetical adsorbent surface that contains only one type of adsorption site (site A) and no pore volume as show in Figure 2(b).

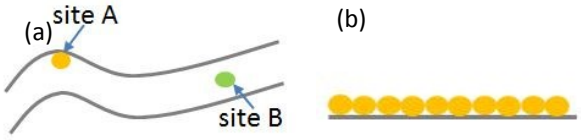

Figure 2: (a) an adsorbent that contains two different types of binding sites, one on the surface (site A) that bounds the pore volume and another one located at the middle of the pore volume (site B); (b) a hypothetical and perfectly homogeneous adsorbent surface that contain only one type of adsorption site (site A).

If it is assumed that a target molecule experiences the same amount of binding energy with these sites at infinite dilution, then all these adsorption sites have equal probability to become occupied by the target molecule. However, if the concentration of the target molecule is increased in the bulk fluid, the adsorption scenario increases in complexity. Even for the Langmuirian adsorption which always happens in a homogeneous adsorbent, adsorption progresses via a gradual increase on the adsorption surface with respect to the concentration of the solute in the bulk solution. For the simplest case of adsorption of a gas molecule onto a perfect and homogeneous graphene surface, the gas molecule fills the surface gradually upon an increase in pressure. If we define a homogeneous surface as a surface that contains only one type of binding site, then for a fixed pressure, p, the gas molecule should cover all the sites available on that surface at that particular pressure. Obviously, this observation cannot be experimentally realized or theoretically demonstrated.

For example, under equilibrium conditions, at infinite dilution, only the most preferential adsorption sites can bring specific target molecules from their bulk phase to an adsorbed phase. Similarly, an adsorption site with a lower binding energy can concentrate the same target molecule but at a relatively higher pressure or concentration. This can be correlated with energy associated with target molecules in the bulk phase. At a higher concentration, an adsorption site is more likely to interact with more target molecules than at a lower concentration. Additionally,

View Article Online
DOI: 10.1039/C9TA00287A

the entropy involved in the bulk phase, which contains a larger concentration of target compound, is lower than the entropy of the bulk phase, which contains a lesser concentration of target compound. Thus, at equilibrium, the energy required to concentrate the target molecule from a bulk phase with a lower entropy is comparatively lower than the energy required to concentrate the target molecule from a bulk phase with a higher entropy (or lower concentration of target molecules). A homogeneous adsorption corresponds to an adsorption system where the balance between the decrease in the bulk phase entropy(entropy penalty) and the energy required to concentrate the target molecule from the bulk phase to an adsorbed state, adjusts in a way so that that the adsorbent and adsorbate interacts with the same level of binding energy, irrespective of the concentration of target molecule in the bulk phase in the adsorption isotherm.

The binding energy associated with the homogeneous adsorption of a target molecule can be defined by a simple analytical expression:

$$q_h(C_e) = \sum_{i=1}^{i=n} N_i \varepsilon_i C_e \quad , \qquad (1)$$

Where, q_h is the amount adsorbed in a homogeneous adsorbent, N is the number of adsorption sites with a binding energy ε and C_e is the concentration of the target molecule at equilibrium. The suffix i corresponds to number of different types of binding sites available on the adsorbent surface. If $i = 5$, this means that the adsorbent surface contains five different types of binding sites and each site will be associated with a certain level of binding energy. The amount adsorbed in such an adsorbent can be written as:

$$q_h(C_e) = N_1\varepsilon_1 C_{e1} + N_2\varepsilon_2 C_{e2} + N_3\varepsilon_3 C_{e3} + N_4\varepsilon_4 C_{e4} + N_5\varepsilon_5 C_{e5} \quad . \qquad (2)$$

The expression in Eq (1) simply represents the amount adsorbed on to the homogeneous surface. This is the summation of the number of adsorbate molecules on to adsorption sites that are associated with different binding energies. N_1 is the number of adsorption sites occupied by the target molecule at an equilibrium concentration of C_{e1}, and each of these binding sites are associated with a specific amount of binding energy, ε_1. For the case of homogeneous adsorption, the energy associated with the different types of adsorption sites will be approximately equal to each other (i.e., $\varepsilon_1 = \varepsilon_2 = \varepsilon_3 = \varepsilon_4 = \varepsilon_5$). However, these adsorption sites can each host the target molecule at different concentrations (e.g., $C_{e1} > C_{e2} > C_{e3} > C_{e4} > C_{e5}$). A type 5 adsorption sites can bring the adsorptive molecule from its bulk gaseous state to the adsorbed state at higher pressures (low entropy in the bulk phase) and the adsorption energy involved will be approximately equal to ε_5. Likewise, a type 1 adsorption site can bring an adsorptive molecule from a highly diluted bulk gas (high entropy in the bulk phase) with an adsorption energy equivalent to ε_1. Nevertheless, the adsorption energy involved on an average scale will be the same due to the homogeneous nature of the adsorbing surface.

For the case of adsorption on to a heterogeneous surface, the binding energy associated with different types of adsorption sites significantly vary. In mathematical form, the amount adsorbed

View Article Online
DOI: 10.1039/C9TA00287A

on to a heterogeneous surface that contains five different types of adsorption sites can be written as:

$$q_{h*}(C_e) = N_1\varepsilon_1 C_{e1} + N_2\varepsilon_2 C_{e2} + N_3\varepsilon_3 C_{e3} + N_4\varepsilon_4 C_{e4} + N_5\varepsilon_5 C_{e5} \quad (3)$$

where, $\varepsilon_1<\varepsilon_2<\varepsilon_3<\varepsilon_4<\varepsilon_5$ and $C_{e1}> C_{e2}> C_{e3}> C_{e4}> C_{e5}$

Figure 3 shows the adsorption isotherm of an adsorptive gas molecule on a perfectly homogeneous surface such as a graphene surface and also on a heterogeneous surface. This is to demonstrate possible adsorption energies involved at five different pressures. For the case of homogeneous adsorption, the adsorption isosteric heat (this concept is later discussed in detail) is independent of pressure or surface loading. However, during the adsorption of a target molecule on a heterogeneous surface, the isosteric heat gradually decreases with an increase in loading or pressures. To demonstrate the concept of homogeneous adsorption, we show molecular graphic snapshots of methane adsorbed on to an ideal pristine graphene surface at 303 K (Fig 3b). Also shown are the molecules in the less dense state in the bulk phase, and the entropy of the bulk gas at those pressures. These snapshots clearly depict the principles behind the homogeneous adsorption. The higher the pressure, the higher the surface coverage and most of the surfaces can be titrated with the target molecule only at the expense of higher pressure. Irrespective of this scenario, the corresponding adsorption isosteric heat required to bring the molecules from the less dense bulk state to a dense adsorbed state is always around 12 $\pm$ 0.5 kJ/mol; [36]this means the surface is homogeneous. This indicates that a homogeneous adsorption does not simply imply adsorption occurring at only one type of binding site (like site A in Figure 2b) but rather that homogeneous adsorption refers to a scenario where the adsorption occurs on a collection of adsorption sites which can individually host a new target molecule at different pressure or concentration. However, the forces required to bring the less dense target molecules (in the gas or liquid phase) to a more dense adsorbed state at different pressures or concentrations, are associated with a specific and almost same level of binding energy.

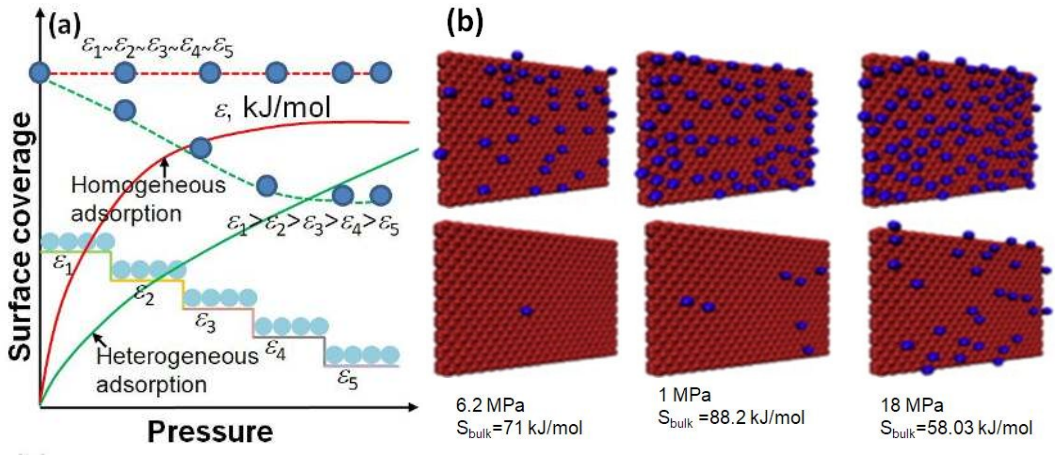

View Article Online
DOI: 10.1039/C9TA00287A

Figure 3: (a) Adsorption isotherm of a target molecule on a homogeneous surface that contains five types of binding sites (this may be the different functional groups, surface curvature, pore volume distribution, etc; shown by continuous red line) and on a heterogeneous surface that contains five different types of binding sites (shown by continuous green line). Also shown are their associated adsorption isosteric heat (indicated by either dotted red for adsorption on homogeneous surface or green lines for adsorption on a heterogeneous surface). (b) Snapshots of methane adsorbed on to a perfectly homogeneous pristine graphene surface (Top panel) at three different pressures and their bulk gas (lower panel; the entropy of the gas molecules in the bulk fluid is shown in parenthesis).The snapshots are taken from the work of Mosher *et al.*;[37]the entropy of the bulk phase was obtained from the NIST fluid webpage.

Eq (1) to (3) and the above discussions are given here only to define the basic concepts behind adsorption in homogeneous and heterogeneous surfaces and to introduce the concept of binding energy and how this relates to homogeneous and heterogeneous surface on the most basic level. It is not necessary that the adsorption isotherms should be (multi) linear as shown in these expressions and, in fact, most of the experimental equilibrium data exhibits a non-linear relationship between the concentration or pressure and the amount adsorbed. Additionally, the type and number of adsorption sites and their associated binding energy required to concentrate the target molecule are typically not known a priori; thus, some initial estimates are required before running any iterative procedures while solving these expressions. A reliable approach to obtain the number of adsorption sites and the types of adsorption sites and the associated binding energy for a specific target molecule can be easily predicted directly from the experimental equilibrium data or from the theoretical adsorption isotherms. Theoretical adsorption isotherms implicitly connect the number of adsorption sites, their binding energy and how they are distributed on an adsorbent surface. As shown in the following section, if the theory is properly exploited along with the assumptions behind the theoretical adsorption isotherm, then the empirically determined isotherm parameters can be used to expose the energetic character of the adsorbent.

3. Characterization of the adsorption site binding energy using adsorption isotherms and the discrete binding model

The simplest equation for predicting the binding energy of a homogeneous adsorbent for a specific target molecule is given by:[38]

$$q_h = \frac{NKC_e}{1 + KC_e} \quad . \qquad (4)$$

For the case of gas adsorption systems, C_e should be replaced by the pressure, p at equilibrium. Eq (4) is the Langmuir adsorption isotherm most widely used to represent the equilibrium adsorption of several pollutants in liquid phase or gas phase onto a wide range of porous materials. q_h refers to the amount adsorbed) onto a homogeneous adsorbent or a homogeneous surface. The parameter N represents the number of adsorption sites and the K is related to the binding energy. According to Eq (4), irrespective of the concentration of the target molecule, the entire adsorption process at equilibrium is associated with a binding energy that is constant and

View Article Online
DOI: 10.1039/C9TA00287A

is equal to *K*. Recalling the concept of the binding energy defined in Eq (1), the amount adsorbed at equilibrium C_e is associated with the same level of binding energy over a range of initial concentrations of the target molecule. In the case of a heterogeneous adsorption surface, the same expression can be used to reveal the energetic heterogeneity of the material. In the case of adsorption on a heterogeneous surface, the Langmuir isotherm can be used to describe the energetic heterogeneity by assuming the adsorbent surface consists of a collection of locally homogeneous surfaces that can be described by a so-called local adsorption isotherm that follows Eq (1).

If an adsorbent contains three different types of binding sites of concentration, N_1, N_2 and N_3, then the Langmuir expression, which assumes uniform site energy on the surface, can be written as: [39]

$$q = q_{h1} + q_{h2} + q_{h3} = \frac{N_1 K_1 C_e}{1 + K_1 C_e} + \frac{N_2 K_2 C_e}{1 + K_2 C_e} + \frac{N_3 K_3 C_e}{1 + K_3 C_e} \quad . \tag{5}$$

Since the Langmuir isotherm represents local homogeneous surface, it is commonly referred to as the local Langmuir model. In Eq (5), q_{h1} represents the amount adsorbed on to adsorption sites of type 1. The constantsN_1, N_2 and N_3 and K_1, K_2 and K_3 can be obtained using simple regression analysis.

Traditionally, the equilibrium constants involved in the Langmuir isotherm (Eq 4) is predicted by linearizing the expression in Eq (1) as follows:[40]

$$\frac{C_e}{q_h} = \frac{1}{KN} + \frac{C_e}{N} \tag{6}$$

and

$$\frac{1}{q_h} = \frac{1}{KNC_e} + \frac{1}{N} \tag{7}$$

Using these expressions, the number of binding sites, *N*, and their binding energy can be obtained via a linear regression analysis from the plot of C_e/q_h versus C_e or $1/q_h$ versus $1/C_e$. Expressions, Eq (6) and Eq (7) can produce tempting straight lines and thus classify the uptake of several pollutants on to a wide range of adsorbents as a homogeneous adsorption process.[41–43]
Though Eq (6) and Eq (7) can provide an easy solution for the design of batch adsorption systems,[44,45]theydo not provide the actual information on the interactions that exist between the different binding sites and the target molecules. Additionally, it is less likely that materials like activated carbon exhibit a homogeneous adsorption of target molecules on their.[46] Thus in-order to expose the natural heterogeneity of the adsorbent surface which hosts the target molecule, it is essential to rewrite Eq (7) as follows:[47]

View Article Online
DOI: 10.1039/C9TA00287A

$$\frac{q_h}{C_e} = KN - Kq_h \quad . \qquad (8)$$

Eq (8) was originally proposed by George Scatchard in order to estimate the affinity parameter involved during the attraction of small molecules and ions by proteins. For the case of adsorption systems, the plot of q_h/C_e versus q_h can provide valuable information on the energetic heterogeneity such as how many types of adsorption surfaces there are for a specific target molecule and their associated binding energy. The plot of q_h/C_e versus q_h also avoids the limitations of the most frequently used expressions (eq6 and eq7) which in most cases oversimplifies the entire adsorption process and classifies most of the adsorbent surface as homogeneous.

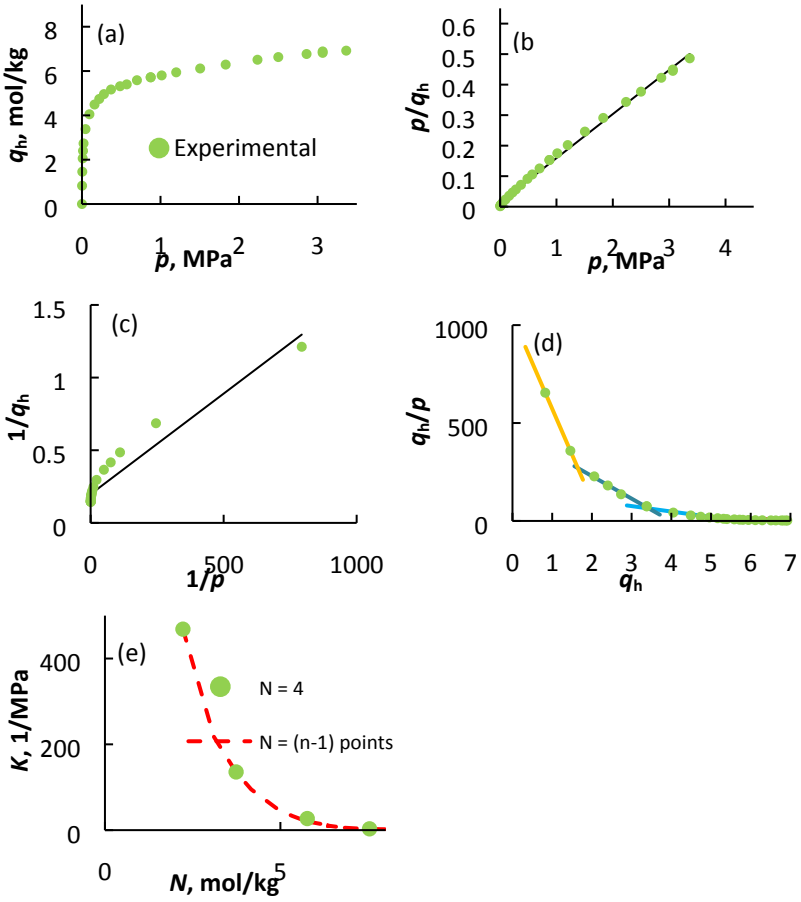

Figure 4: (a) Adsorption isotherm of CO_2 on to zeolite 13x (experimental data taken from the works of Alirio et al.[16]), (b) experimental data and the fitted Langmuir isotherm based on the plot of p/q_h versus p, (c) experimental data and the fitted langmuir isotherm based on the plot of $1/q_h$ versus $1/p$ (d) experimental data and the fitted langmuir isotherm according to a Scatchard equation, and (e) Binding site affinitiy spectra obtained based on the Scatchard plot method that assumes there are four different types of active sites and (n-1) type of active sites.

View Article Online
DOI: 10.1039/C9TA00287A

A plot of amount of CO_2 adsorbed on to zeolite 13x versus the equilibrium pressure is shown in Figure 4. In Figure 4b and 4c, the predicted relation between q_h versus p based on Eq (6) and Eq (7), respectively are shown. It can be observed that transposing the adsorption equilibrium data in Figure 4b and 4c can provide a misleading linear relationship between q_h/p versus q_h or $1/q_h$ versus $1/p$. However, if we look at the equilibrium data fitted using a Scatchard equation, at least four distinct regions can be observed (Figure 4d). This essentially indicates, according to the Scatchard equation, that the adsorbent contains at least four different types of adsorption sites with corresponding binding energies ofK_1, K_2, $K_3$and K_4. Depending on the number of distinct regions that can be observed in a Scatchard plot, it would be easy to predict or characterize the heterogeneity of the adsorbent. Despite the advantage of this method to rapidly discriminate the type and number of binding sites, it also has disadvantages. As mentioned earlier, the number of adsorption sites and their associated binding energies required to concentrate the target molecule are typically not known a *priori* and thus a preliminary assumption is needed. Also, this method is sensitive to the number and position of the tangents drawn in the Scatchard plot (in Figure 4e we drawn up to 4 tangents and obviously more tangents could be drawn depending on the data interpretation). One method to avoid this limitation is to split the binding model into (n-1) Langmuir isotherms; where n, is the number of points in the adsorption isotherm. In this way, it is possible to obtain the slope and intercept of the linear trend line that consecutively connects each pair of experimentally determined points in the Scatchard plot (Figure 4e). In Figure 4e, the plot of the number of binding sites, N versus their binding energy is shown. The Scatchard plot reasonably produces the site energy distribution. The accuracy can be improved by obtaining the amount adsorbed at equilibrium over a wide range of initial concentrations of the adsorbate. This method is also reliable since the binding site energies and their distribution is measured within an analytical window, which depends on the minimum and the maximum p or C_e value in the experimental adsorption isotherm (see Figure 4a). This approach of estimating or characterizing the binding energy based on the assumption that a heterogeneous surface consists of a finite number of different kinds of adsorption sites is one of the oldest approaches and is conceptually referred to as a discrete binding model.

4. Homogeneous versus heterogeneous surface

The definition of a homogenous and a heterogeneous surface can be based on the type of adsorption involved. Both of these adsorption types can be defined from the principles of potential energy or a potential function that can be taken as a measure of the interaction energy of an isolated molecule with the adsorbent. The adsorption site simply corresponds to a specific point on the adsorbent surface or a local area that can bring the adsorbate molecule from the bulk of the fluid to an adsorbed state via strong chemical forces or through comparatively weaker physical forces. Thus, the adsorption energy is usually defined as the average energy of the molecules in the bulk phase to the minimum potential energy at which the molecule in the bulk phase are brought into a less mobile or otherwise adsorbed state. Theoretically, the molecules vibrate and move randomly in the bulk phase, whereas in an adsorbed state, the molecules are trapped in the adsorption sites and thus the translational/vibrational motion of the adsorptive molecules are at the point of (local energy) minimum.

View Article Online
DOI: 10.1039/C9TA00287A

According to the principle of potential energy, the potential energy function, $U(x, y, z)$ is related to the force acting on a particle; where x, y and z are the cartesian coordinates of the adsorbed molecule. The force acting on the adsorbent molecule due to any atom or adsorption site on a planar adsorbent surface (x,y – plane) can be related to the derivative of the potential energy, $U(z)$; [48]

$$F(z) = -dU(z)/dz \quad , \qquad (9)$$

where,z is the perpendicular distance between the particle and the surface or an adsorption site on the surface.

Thus the potential energy can be obtained by simply integrating the above expression as follows:

$$U(z) = -\int F(z).dz \qquad (10)$$

The negative sign indicates the force is always directed in such a way that the particle moves towards a lower potential energy. The steeper the $U(z)$, the stronger the force or the adsorption energy is. This concept is demonstrated in Figure 5afor a planar surface. The term $3/2kT$ in Figure 5 presents the average kinetic energy of a particle in motion in three dimensions. As mentioned earlier, the adsorption forces also include the energy involved in bringing the highly mobile gas phase to an adsorbed state. The potential energy, $U(z)$ itself is not conserved: when the particle moves, the $U(z)$ also varies. Thus, during adsorption or, in general, during the interaction between any two molecules or atoms in a molecule, what is conserved is the total energy i.e. the sum of potential and kinetic energy, which includes the contribution of the kinetic energy associated with the energy of the gas. The loss of kinetic and potential energy during the adsorption of molecule on an adsorption site corresponds to the differential heat of adsorption. An additional energy is required to enable the adsorbed molecule overcome the potential energy barrier that keep the adsorbed molecule in adsorbed state and to partly restore the kinetic energy required to confer the degrees of translational and rotational freedom that pertain to the gaseous state.

The concept of potential energy objectively helps to define the molecular state of the adsorbed species. The adsorbent surfaces can be characterized using the potential function, U. According to Figure 5a, the potential function for adsorbent surfaces is defined as the difference between potential energy per mole for adsorption of a molecule in the gas phase, $gP^{ads}$and the average vibrational energy per mole of a molecule in the adsorbed state, aE^{vib}. In the case of adsorption, typically an adsorbed molecule is capable of free translation parallel to the surface and vibration normal to the surface, associated with an average vibration energy, aE^{vib}. At 0 K, this value approaches a value of $aE_o^{vib}$and at higher temperatures, aE^{vib}approaches RT. Thus, the function $U(z)$ defined in Eq (10) is always temperature dependent because of the vibrational energy which depends on temperature. If the point at which the adsorbed molecule possesses a zero energy (commonly referred to as the zero-point energy of the adsorbed molecule) is known, it is possible to obtain the absolute adsorptive potential, U_o which is independent of temperature. U_o is simply the difference between the potential energy per mole for adsorption of a molecule in the gas

View Article Online
DOI: 10.1039/C9TA00287A

phase, $gP^{ads}$and aE_o^{vib}. A basic understanding of the energy parameters shown in Figure 5a is absolutely essential to estimate the adsorption forces and to understand the concept of binding energy and the surface properties of adsorbents. For this purpose, the typical potential well for adsorbate-adsorbent interactions and their relationship to the different heats of adsorption is shown in Figure 5a (this figure was adapted from the one of the works by the pioneers in adsorption, Olivier and Ross[49]). According to Figure 5a, the differential heat of adsorption, q_{diff} measures the energy required to remove an adsorbed molecule from its average vibrational state and from the attractive forces of its adsorbed neighbors to an infinite distance from the surface, plus the energy equivalent to the degrees of freedom of the molecules of the gas in the excess to that of the adsorbed gas.

Depending on the variation of U_o on the adsorbent surface, it is possible to classify adsorbent surfaces in to different categories as shown in Figure 5b-g. [50,51]

(a) Heterogeneous periodic surface: If the surface is characterized by the presence of different minimaU_{o1}, U_{o2}, ..,U_{on}, then it can be classified as a heterogeneous surface (see Figure 5b). If the different minima repeat and if they are separated by a specific amount of distance, then it is called a periodic heterogeneous surface. Usually these surfaces contain a discrete number of binding sites. One simple example is adsorption of a H_2 molecule in mesoporous silica whose surface heterogeneity is characterized by the presence of at least two different types of atoms on the surface. A H_2 molecule (or any other adsorbate) will experience a different level of binding energy with the Si and O atoms and also will experience a different level of binding energy at the middle of the mesopore; however the structure itself is periodic in three-dimensions.

(b) Completely random and heterogeneous surface: If the surface is characterized by the presence of several minima, U_o, occurring randomly and spread over the adsorbent surface, then such surfaces can be classified as completely random and heterogeneous(Figure 5c).The target molecule will experience a wide range of different binding energies on the surface that differ from a few to hundreds of J/mol and these sites will selectively host a target molecule at different temperatures and pressures or concentrations. Depending on the bulk pressure at which these sites host the target molecules, the adsorbent sites can be titrated with the host molecule and the surface properties can be characterized (see Section 2). Biomass derived carbons and many porous amorphous carbons that seem to contain a wide range of pore-size distributions with different types of functionalities like N, -OH, -COOH groups, together with the presence of any impurities,[52] can ultimately possess characteristic properties of a random and heterogeneous surface. Even porous polymers can fit under this category depending on the distribution of pore-size and pore-volume and presence of functionalities, if any.

(c) Homotattic surface: An adsorbent surface can contain different submicroscopic patches or regions of regular and uniform construction;[53] each of these patches is a homogeneous surface (Figure 5d). A classic example would be the adsorption of a crystallizing compound in its own solution or an adsorption of an impurity molecule onto a crystallizing compound. An adsorptive molecule will experience the same level of interaction with one of the faces of the crystal, whereas it will experience a completely

View Article Online
DOI: 10.1039/C9TA00287A

different level of binding energy on the other face of the crystal. In other words an adsorbent surface will contain different patches of surfaces, while each of these faces can be considered as energetically homogeneous. Where such material is frequently encountered is in carbon structures where the homotattic surface may be evident by the virtue of regularities on the pore surface rather than by crystallographic regularities. Some examples include carbon foams and[54,55] pillared graphene,[56] where the structure contains different homotattic patches. In the case of carbon foams this is the parent nanotubes which make the carbon foams and in the case of pillared graphene, at least two homogeneous surfaces can be expected, one is the graphene surface itself and the other one is the surface of carbon pillars that separate two graphene layers by a certain distance. Another example includes metal organic frameworks with bimodal or trimodal pore size distribution. If the surface chemistry is ignored and it is assumed that the interaction potential is uniform within those pore volumes, then each of the pores that differ by size can be taken as homotattic surface patches.

(d) A completely homogeneous surface: Every point or every location on the perfectly homogeneous adsorbent surface experiences the same level of binding energy with the adsorptive molecule. On such a homogeneous two-dimensional surface, with $U(x,y)$ at a given z_o, U_o is a constant (Figure 5e). One example is the hypothetical smooth surfaces that are commonly assumed in the theoretical modeling of adsorption of small molecules (H_2, CH_4, N_2 and CO_2) on graphene-based porous materials like 2D graphene sheets or carbon nanotubes.

(e) Homogeneous periodic surface: Theoretically, temperature plays a major role in bringing the molecule from its average vibrational state or from its bulk phase to an adsorbed phase. At lower temperatures, it is easier to bring the molecules to an adsorbed state. In the case of a planar surface, depending on the oscillations in $U(z)$ at a temperature, kT, it is possible to characterize and classify the adsorbent surfaces into a homogeneous periodic surface or homogeneous periodic site surface. If the two-dimensional planar surface contains a periodic molecular structure, then on such a surface, if the oscillations in U_o are much lower than kT, the surface can be regarded as a homogeneously periodic surface (see Figure 5f). One typical example is the adsorption of CH_4 on a graphene surface. The potential energy of hexagon ring centers is lower than the ring edges. Earlier Gubbins showed in such a system methane sits at the centers of the alternate hexagons.[57]

(f) Homogeneous periodic site surface: If the two-dimensional planar surface contains a periodic molecular structure and if the oscillations in $U(z)$ is exceedingly higher than kT, then the locations on the surface where potential is at minimum, U_m are usually called adsorption sites or adsorption centers. On homogeneous periodic surfaces, the local minima can be the same and are equal to U_m. Adsorptive molecules can be adsorbed on to these sites and the difference between the energy of these minima and the average energy of the molecules in the equilibrium bulk state is the energy of site adsorption. Example systems can be a simple crystalline adsorbent made up of two atoms types (A and B) separated by some distance. If the oscillations in U with respect to site A are much less than kT, whereas the oscillations in U with respect to site B are much higher than kT,

View Article Online
DOI: 10.1039/C9TA00287A

the local minima will be located on the adsorbent surface separated by a distance that will be equal to the distance between two neighboring B atoms (see Figure 5(g)). Many metal organic frameworks will fit under this category, especially at lower pressures, where the gas molecules will be preferentially adsorbed on to the metal nodes separated by a fixed distance. Such a scenario can be taken as a representative example of a homogeneous periodic surface. Obviously at higher pressures, this scenario will be different as the guest molecules can adsorb on to the surfaces of linker molecules before complete pore filling.

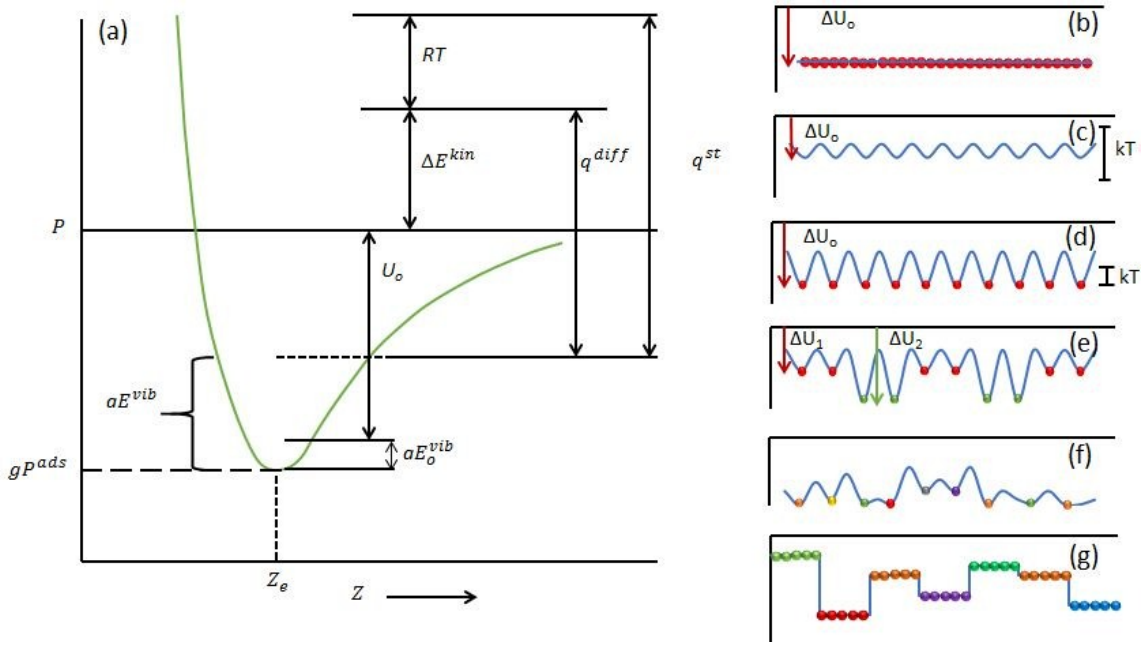

Figure 5: (a) variations of the potential energy, ΔU° across the surface of an adsorbing solid: (b) heterogeneous periodic site surface, (c) completely random heterogeneous surface, (d) homottatic heterogeneous surface, (e) perfectly homogeneous and smooth surface, (f), homogeneous periodic surface and (g) homogeneous periodic site surface. The types of the adsorption surfaces were drawn based on the images described in the works of Rudzinski.[51]

5. Limitations of the discrete binding model

Based on the above discussed definitions, it can be realized that empirically classifying the surface heterogeneity into a specific number and type of binding sites is not straight forward. For instance, it would be extremely difficult to classify a material containing surfaces that can be treated with a simple bi-Langmuir or tri-Langmuir isotherm or a multi-site Langmuir isotherm of infinitely large number of sites with different energetics. Several initial assumptions or prior knowledge about the material are also required, say for example about their pore properties or surface chemistry, etc. These are the common disadvantages of the discrete binding model. For instance, the number or type of the sites can be simply varied by varying the number of tangents drawn on the Scatchard plot (Figure 4e). This may be a useful strategy for a heterogeneous periodic surface. However, for the material with energetic heterogeneity detailed in Figure 1a and Figure5c, there is no straightforward technique to give prior information about the types of

View Article Online
DOI: 10.1039/C9TA00287A

adsorption sites located on the adsorbent surface; in some cases information will be lost during the linearization. Instead of a few homotattic patches (say for e.g., five different types of adsorption sites), the adsorbent surface will contain different types of adsorption sites and in that case the heterogeneity can be characterized by a continuous distribution function of adsorption energies. Such mathematical functions are commonly called affinity distribution functions (ADFs). This will simply negate the limitations of the Scatchard plot method since this method does not require any prior assumptions on the number/type of binding site for a specific molecular probe.

6. Affinity distribution function

The affinity distribution function is a continuous distribution function that obtains the adsorption site energy spectrum, which correlates the adsorption isotherm parameters with energetic parameters.[50]ADFs can approximate the energetic heterogeneity of the adsorbent surface within an analytical window that can be quantitatively compared or measured for a wide range of adsorbents for a specific target molecule. Such functions are represented in a plot of binding sites versus their binding affinity or binding energy. Such functions simultaneously provide a quantitative measure of the number of the binding sites with respect to their binding energy for a target molecule, and also a measurement of the degree(this will be discussed in detail later) of the heterogeneity.

Such a mathematical function can be derived from the basic integral equation that represents the adsorption on heterogeneous surfaces;[26,50]

$$q_e(C_e) = \int_{i=0}^{i=\infty} q_h(C_e,E).F(E).dE \qquad . \qquad (11)$$

According to eq. (11), the total adsorption of a heterogeneous surface, $q(C_e)$ is the integral of adsorption on a homogeneous surfaces that can be represented by an energetically homogeneous isotherm(q_h) multiplied by a frequency distribution $F(E)$ over a range of energies, E. $F(E)$ can be defined as the differential distribution of the surface area that has binding energies over a range of values of E. The number of sites, i, is the physical domain of the adsorption site energies that exist at the adsorbate-adsorbent interface. The limits of the integral of the adsorption energy can range from zero to infinity. Their range can be approximately assigned based on the minimum and maximum adsorption energies, which are again, are not known *a priori*. Later we will show how the adsorption energies can be reasonably approximated for a heterogeneous adsorption system from the studied range of adsorbate concentration, or based on the C_e values in the adsorption isotherm. Theoretically the adsorption sites on the adsorbents can be treated using a discrete model such as bi or tri-Langmuir isotherm. In a material like activated carbon, the energetic heterogeneity is highly dense and therefore can only be approximated by a continuous function.

The amount of adsorbate adsorbed onto a homogeneous surface can be represented by Langmuir isotherm and thus can be used in q_h of Eq (11). As Langmuir isotherm assumes adsorption occurs on adsorption sites that exhibit the same amount of energy, it can be used to represent adsorption

View Article Online
DOI: 10.1039/C9TA00287A

on heterogeneous surface that contain several patches of homogeneous surface or locally homogeneous surfaces. If the number of adsorption sites and their type and their distribution are known or if can be assumed, then the overall adsorption isotherm can be predicted from the adsorption integral in Eq (11). Alternatively, if the adsorption at the solid-liquid interface can be described by a heterogeneous isotherm (such as Freundlich, Freundlich-Langmuir and Redlich-Peterson isotherm), then Eq (11) can be used to predict the energy spectrum or the corresponding site energy distribution. This can be achieved by expressing adsorption isotherm in terms of the energy of adsorption. Cerofolini proposed such a useful method.[58] According to Cerofolini approximation, the true kernel is replaced by a condensation isotherm. This can be done by relating the equilibrium fluid phase concentration to the energy of adsorption using the Polanyi potential theory given by[58,59]

$$p = p_s \exp^{\left(-\frac{E^*}{RT}\right)} = p_s \exp^{\left(-\frac{E-E_s}{RT}\right)} \quad , \qquad (12)$$

where, p_s is the vapor pressure of the gas molecule of interest, E is the lowest physically realizable energy and E_s is the adsorption energy corresponding to p=p_s (vapor pressure of the gas), R is the universal gas constant, T is the absolute temperature and E^* is the net energy.
The equivalent to Eq (12) for the case of liquid adsorption is given by

$$C_e = C_s \exp^{\left(-\frac{E^*}{RT}\right)} = C_s \exp^{\left(-\frac{E-E_s}{RT}\right)} \quad . \qquad (13)$$

where, C_s is the maximum solubility of the solute in the solvent, E is the lowest physically realizable energy, E_s is the value of the adsorption energy when C_e = C_s.

Substituting Eq (12) or (13) in Eq (11) will lead to an approximate site energy distribution, $f(E^*)$ which is the differentiation of the isotherm, $q(E^*)$, with respect to E^*:

$$f(E^*) = -\frac{dq(E^*)}{dE^*} \quad . \qquad (14)$$

Equation (14) can be used to determine the site energy distribution function by differentiating the corresponding isotherm expression with respect to E*. As the site energy distribution defined in Eq (14) is not normalized, the area under the distribution curve typically will give the maximum adsorption capacity, q_m, given by:

$$q_m = \int_{E^*_{min}}^{E^*_{max}} \frac{dq(E^*)}{dE^*} \qquad (15)$$

$E^*_{min}$and$E^*_{max}$are the limits of energy space that are directly related to the maximum and minimum pressure in the adsorption isotherm (see Figure 6), respectively.

View Article Online
DOI: 10.1039/C9TA00287A

$$E^*_{min} = -\ln\left(\frac{p_{max}}{p_s}\right)RT \quad (16)$$

$$E^*_{max} = -\ln\left(\frac{p_{min}}{p_s}\right)RT \quad (17)$$

Since Eq (14) has no mathematical restrictions, it can predict negative energy values when $E<E_s$, which has no physical meaning. Irrespective of the adsorption system site energy distribution spectra can be estimated for values of $E^* = 0$ to $E^* = \infty$. Alternatively, more precise (see the shaded regions in Figure 6) and theoretically meaningful site energy spectra can be obtained using the minimum and maximum pressure observed in the experimental adsorption isotherm. In Figure 6we show the relation between the adsorption pressure and the net adsorption energy. In fact, as the isotherm parameters are sensitive to the pressure range covered and the shape of the adsorption isotherm, only the energy distribution obtained within this pressure (or concentration) range can be considered valid.

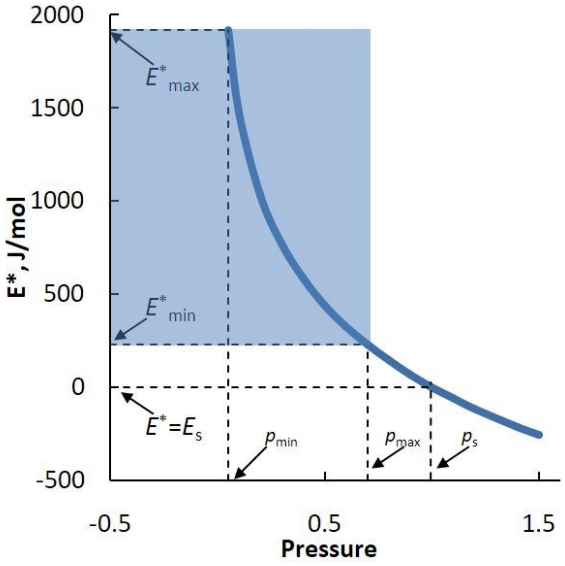

Figure 6: Relation between the adsorption pressure limits and the net adsorption energy (blue shaded regions represent the analytical window where a meaningful adsorption site energy spectrum can be obtained using the condensation approximation method).

The site energy distribution of any theoretical isotherm can be obtained by substituting the value of pressure or concentration in the adsorption isotherm with Eq (12) or Eq (13) and then differentiating the resulting expression with respect to E^* according to Eq (14). Such expression can also be used to estimate the characteristic energetic distribution of any theoretical isotherm. Below we give the most widely used Langmuir-Freundlich (LF) isotherm (Eq (18)) and its site energy distribution function predicted using the condensation approximation method.[60]

$$q = q_m\left[\frac{bp^n}{1+(bp)^n}\right] \quad (18)$$

View Article Online
DOI: 10.1039/C9TA00287A

b and *n* in the above expression are called Langmuir-Freundlich constants and are related to the maximum adsorption capacity and heterogeneity of the adsorbent.

$$f(E^*) = \frac{q_m n (bp_s)^n}{RT} \exp\left(\frac{-nE^*}{RT}\right)\left[1 + (bp_s)^n \exp\left(\frac{-nE^*}{RT}\right)\right]^{-2} \quad (19)$$

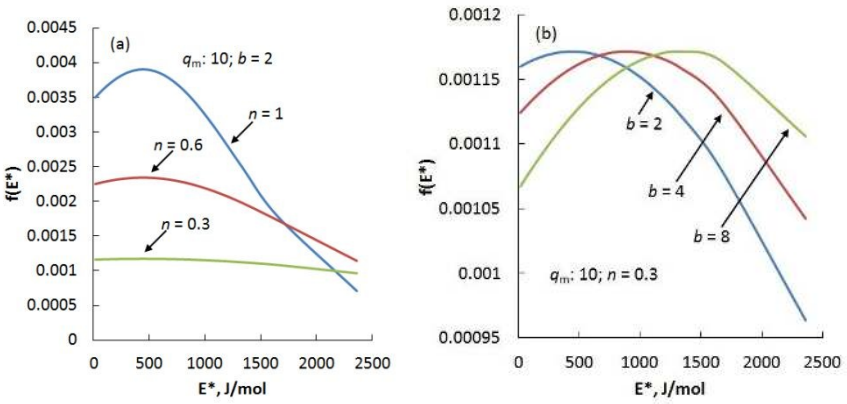

Figure 7: Site energy distribution function, $f(E^*)$ according to Langmuir-Freundlich isotherm for different assumed values of the isotherm constants *b* and *n* (the maximum adsorption capacity, q_m is fixed and is assumed to be equal to 10).

In Figure 7, we show the site energy distribution spectra constructed using the above expression based on some assumed values for the isotherm constants, q_m, *b* and *n*. Eq (19) gives a quasi-Gaussian site energy distribution, which is exactly the distribution of the Langmuir-Freundlich isotherm. For *n* = 1, according to Eq (19) the Langmuir-Freundlich isotherm exhibits a quasi-Gaussian distribution of binding site energies. For lower values of *n*, Langmuir-Freundlich isotherm exhibits a more exponential distribution of site energies especially at lower pressures. Another notable feature is that the mean energy (for fixed values of *b* and q_m) is not significantly influenced by the value of *n*. The higher the isotherm constant, the narrower the site energy distribution and the higher the mean energy. For lower values of *b* and *n*, adsorption energies are exponentially distributed (not shown in Figure 7). Figure 7shows how the condensation approximation method can be used to extract theoretical insights from an adsorption isotherm like the LF isotherm. This method can be used to underpin the theoretical background of any empirical or semi-empirical or theoretical adsorption isotherms.

For instance, the site energy distribution function of the generalized Freundlich isotherm (Eq (20)) and the commonly used Freundlich isotherm (Eq (21)) can be obtained using the condensation approximation method and are given in Eq (22) and Eq (23) respectively.[61]

$$q = q_m\left[\frac{bp}{1+bp}\right]^n \quad (20)$$

View Article Online
DOI: 10.1039/C9TA00287A

$$q = q_m b p^n \tag{21}$$

$$f(E^*) = \frac{q_m n (bp_s)^n}{RT} \exp\left(\frac{-nE^*}{RT}\right)\left[1 + (bp_s)\exp\left(\frac{-E^*}{RT}\right)\right]^{-(n+1)} \tag{22}$$

$$f(E^*) = \frac{q_m n (bp_s)^n}{RT} \exp\left(\frac{-nE^*}{RT}\right) \tag{23}$$

Eq (23) exhibits an exponential distribution of the binding site energies, which agrees with the theoretical assumptions of the original Freundlich isotherm. In the case of generalized Freundlich isotherm, the approximate site energy distribution function produces a quasi-Gaussian type of distribution widened toward higher values thus partially retaining the exponential type of distribution over a wide range of adsorption pressures.

Eq (18, 22, and 23) can be used to characterize the adsorbent materials that are commonly employed for the storage of gas molecules like CO_2, H_2 and CH_4 or separation of these mixtures. From the value of the isotherm parameters, q_m, n and b it is possible to estimate how the binding site energies are distributed. Likewise, these expressions can be used to interpret the experimental equilibrium data of several pollutants adsorbed from wastewater or from their aqueous solutions. For instance the performance of the adsorbents can be compared using the mean energy and distribution of the site energies. Kumar *et al*[27]used this method to identify the structural differences in the activated carbons prepared from a same precursor by at different experimental conditions and also to estimate the site energy distribution of activated carbons that contains same pore properties but their surfaces doped with heteroatoms. A Toth isotherm showed the adsorption sites are exponentially distributed for the carbon doped with iron or boron heteroatoms. It also showed that the carbon structures with heteroatoms Fe and B reduced both the concentration of highest and lowest energy binding sites. Carter *et al*[61] used the site energy distribution function to monitor the changes in the site energy distributions of that sorbent caused by prior irreversible sorption(preloading) of other solutes. They showed that, based on the affinity distribution functions that regardless of the type of initial site energy distribution assumed, preloading of activated carbon by a non-desorbable solute result in a loss of surface heterogeneity. More importantly, it also detailed what types of sites are lost due to pre-loading. Results demonstrated that the most energetic sites are lost due to pre-loading, with the number of sites in the lowest energy range actually increasing in some cases. This is an important finding and the works of Carter *et al* demonstrates the usefulness of the affinity distribution functions to characterize the effect of one adsorbed solute on the surface heterogeneity of the adsorbent surface to host another guest molecule. Kumar *et al*[62]used the site energy distribution function obtained from a Sips isotherm to model the site energy distribution spectra of a series of activated carbon obtained via chemical activation and the same carbons subjected to physical activation using CO_2 but for different periods of activation time. They showed how the porosity alters the heterogeneity and mean value of the binding energy of the adsorption sites. Through such simple mathematical expressions, they showed that carbons subjected to higher activation time are more heterogeneous and their binding sites are exponentially distributed whereas in the as

View Article Online
DOI: 10.1039/C9TA00287A

obtained carbons after chemical activation, the adsorption energies of the binding sites are uniformly distributed. The method of condensation approximation is sensitive to the theoretical adsorption isotherm used. In fact, there is no universal expression that can reproduce the experimental equilibrium data of different adsorption systems and it is essential to find the site energy distribution function for different adsorption isotherms. In Table 1 of the supplementary file, we listed the commonly used adsorption isotherms and their site energy distribution functions obtained using the condensation approximation method. These isotherms and their site energy distribution functions can be used to expose the heterogeneity of the materials or understand the underlying mechanisms of these theoretical expressions.

7. The method of Stieltjes transforms

Sips proposed a useful method to obtain the distribution of adsorption energies on catalyst surfaces, provided the adsorption isotherm is known, using the method of Stieltjes transform.[34,35] This method assumes that the molecules adsorbed onto the adsorbent surface are in their molecular state, i.e., no dissociation, and also assumes that the heterogeneity is due to the presence of several homottatic surfaces that can described the local or Langmuir adsorption isotherm. If $N(\varepsilon)d\varepsilon$ is the total number of active sites whose adsorption energies per mole lies between ε and $\varepsilon+d\varepsilon$. Assuming the totality of these binding sites can be represented by the Langmuir isotherm, the proportion of the sites of adsorption energy ε covered with molecules is given by:

$$\theta(\varepsilon)d\varepsilon = \frac{N(\varepsilon)d\epsilon}{1+{}^{a}\!/_{p}e^{-\epsilon/RT}} \qquad (24)$$

where, the term θ is a function of p and T, and at constant temperature, it will be a function of the pressure only. p is the pressure and a is a constant which should have the same value for all the sites.

Likewise, the total extent of the covered surface can be obtained by integrating Eq (24) over a whole range of possible values of q that is between $-\infty$to $+\infty$ so that:

$$\theta = \int_{-\infty}^{\infty} \frac{N(\varepsilon)d\epsilon}{1+{}^{a}\!/_{p}e^{-\epsilon/RT}} \qquad (25)$$

where, this value θ can be accurately predicted from the experiments and to date we have a wide range of theoretical isotherms that can explain most of the experimentally observed adsorption isotherms in different class of porous materials. Alternatively, θ can be obtained using a theoretical expression that can fit the experimental adsorption isotherms with high accuracy.

Replacing a/p by y and $\exp(\varepsilon/RT)$ by x, Eq (25) can be written as[34,35]

$$\frac{\theta(a/y)}{RT} = \int_{-\infty}^{\infty} \frac{N(RT.lnx)dx}{x+y} \qquad (26)$$

According to the theory of Stieltjes transform, if we have a function

View Article Online
DOI: 10.1039/C9TA00287A

$$f(y) = \int_{-\infty}^{\infty} \frac{\varphi(x)}{x + y} dx \quad (27)$$

then there exist definite integral for the Eq (27)

$$\varphi(x) = \frac{f(xe^{-\pi i}) - f(xe^{\pi i})}{2\pi i} \quad . \quad (28)$$

If we compare the Eq (27) and Eq (28) with Eq (26), it can be easily realized that the expression on the right hand-side of the Eq (26) is the Stieltjes transform of the function, $N(RT.lnx)$.
The left-hand side of Eq (26) can be substituted with any theoretical isotherm in order to determine the distribution of adsorption energies.

Sips used Eq (29) to determine the distribution of adsorption energies of Freundlich isotherm given by

$$\theta(p) = Ap^c \quad (29)$$

Where, *A* and *c* are Freundlich constants at a fixed temperature. The corresponding distribution of adsorption energies can be determined by substituting Eq (29) and Eq (28) in Eq (27)

$$f(y) = A(a/y)^c = (Aa^c/RT)y^{-c} \quad (30)$$

so that

$$\varphi(x) = \frac{x^{-c}e^{\pi ic} - x^{-c}e^{-\pi ic}}{2\pi i} = \frac{Aa^c sin\pi c}{RT \quad \pi} x^{-c} \quad (31)$$

and

$$N(\varepsilon) = \frac{Aa^c sin\pi c}{RT \quad \pi} \exp(-c\varepsilon/RT) \quad (32)$$

Similar to the condensation approximation method, the method of Stieljtes transform also helps to underpin the distribution of adsorption energies for a given theoretical isotherm. For instance according to Eq (32), the Freundlich isotherm corresponds to an exponential distribution of the active centers. However, this also indicates the limitation of this model. The exponential distribution of active centers cannot be valid for every system as it assumes the amount adsorbed increases exponentially with pressure or in other words the number of available sites is infinite. Despite this limitation, Eq (32) can be used to estimate the adsorption energies of the binding sites of most of the adsorbent/adsorbate systems where low bulk concentrations are involved. In such cases, the adsorbent surface may not reach saturation and in such cases Freundlich isotherm is sufficient to successfully characterize the adsorbent heterogeneity. To support the readers, in

View Article Online
DOI: 10.1039/C9TA00287A

the supplementary file we uploaded the Microsoft excel spreadsheet where we explained in detail how to get the site energy distribution spectra using the Freundlich isotherm according to *the condensation approximation* method.

For systems where, high pressure or high concentration is involved, obviously the adsorbent surface becomes saturated. This means as concentration of sorbent is increased, the amount adsorbed θ asymptotically approaches towards unity. Sips proposed an empirical expression based on the Freundlich isotherm, but it can predict the θ value over a range of pressures or concentrations. Sips expressed the Freundlich isotherm as:

$$\theta = \frac{Ap^c}{1 + Ap^c} \tag{33}$$

If p is small, then $Ap^c << 1$ and the Eq (33) reduce to Freundlich isotherm. For larger p values, θ approaches unity. Though Sips proposed this expression purely based on mathematical terms, to date several experimental works show this expression is accurate enough to predict the adsorption of different molecules from either gas or liquid phase on to different class of porous materials. Sips derived the kind of distribution of active centers according to this expression using the same method of Steiljtes transform.

$$\varphi(x) = \frac{Aa^c\left(\frac{x^{-c_e\pi ic} - x^{-c_e - \pi ic}}{2\pi i}\right)}{1 + Aa^c\left(\frac{x^{-c_e\pi ic} - x^{-c_e - \pi ic}}{2\pi i}\right)} \tag{34}$$

from this, using eq(26), the distribution of adsorption energies can be readily derived

$$N(\varepsilon) = \frac{Aa^c \exp\left(-\frac{c\varepsilon}{RT}\right)\sin \pi c}{1 + 2Aa^c \exp\left(-\frac{c\varepsilon}{RT}\right)\cos \pi c + (Aa^c)^2 \exp\left(-\frac{2c\varepsilon}{RT}\right)} \tag{35}$$

According to the expression, Eq (35), when $\varepsilon \rightarrow \infty$ and $\varepsilon \rightarrow -\infty$, $N(\varepsilon) \rightarrow 0$ and thus $N(\varepsilon)$ is always positive. Thus, there should exist a maximum for a definite value of ε. This can be determined by differentiating Eq (35) with respect and ε and equating it to zero.

$N'(\varepsilon) = 0$

Sips found this maximum corresponds to:

$$\varepsilon = \varepsilon_{max} = (RT/c)\log(Aa^c) \tag{36}$$

Using Eq (36), Sips obtained the following expression:

View Article Online
DOI: 10.1039/C9TA00287A

$$N(\varepsilon) = \frac{1}{\pi RT} \frac{exp\left[\left(\frac{c}{RT}\right)(\varepsilon_m - \varepsilon)\right]\sin \pi c}{1 + 2cos\pi c.exp + exp\left[(\varepsilon_m - \varepsilon)\left(\frac{2c}{RT}\right)\right]} \quad (37)$$

Mathematically, according to Eq (37) the distribution of energetic sites should follow a bell-shaped curve or a Gaussian like distribution. In Figure 8, we show the plot of $N(\varepsilon)$ as a function of $(\varepsilon_m\text{-}\varepsilon)$. It can be observed that for larger value of $(\varepsilon_m\text{-}\varepsilon)$, Eq (37) predicts an exponential type of energetic distribution (see the shaded regions in Figure 8). This means at lower pressures, Eq (37) reduces to a Freundlich type of expression which commensurate with the theoretical background of the Eq (33). Figure 8 also expose the influence of *c* value on the spread of the energetic site distribution. When *c* is equal to unity, the adsorption site energies are more concentrated and not widely spread.

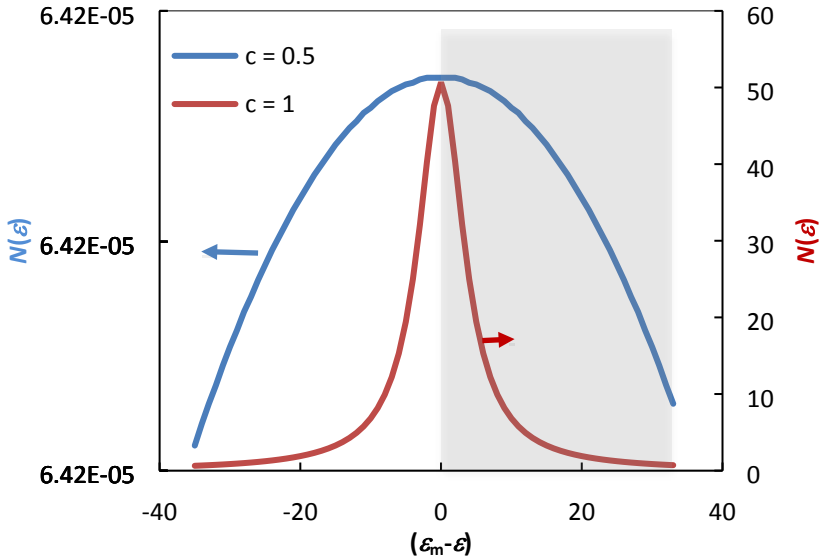

Figure 8: Site energy distribution curve for different assumed *c* values.

It should be noted that negative adsorption energies in Figure 8 do not have any physical meaning and thus the distribution of adsorption energies based on the integration limits from $-\infty$ to $+\infty$ is questionable. Hill[63] pointed out this issue highlighting the non-physical part involved in the statistical distribution of energies of adsorption amongst the active sites on the adsorbent surface. Sips, re-examined his approach and confirmed that a unique distribution function can still be obtained even if one assume the adsorption energies extends from 0 to $+\infty$.[34] Sips showed the adsorption energies of the binding sites follow and exponential trend within the analytical limits that range from zero to infinity.[34]

$$N(\varepsilon) = \frac{1}{RT}\frac{\sin \pi c}{\pi}\left[\exp\left(\frac{\varepsilon}{RT}\right) - 1\right]^{-c} \quad (38)$$

View Article Online
DOI: 10.1039/C9TA00287A

According to Eq (38), when $\varepsilon \rightarrow 0$, $N(\varepsilon) \rightarrow 0$, which has no physical meaning. Sips highlighted this consequence and showed that when ε is very low within the range zero to infinity, the number of active centers is proportional to:

$$\int_{\epsilon=0}^{\epsilon=\infty} \frac{d\varepsilon}{\varepsilon^c} = \frac{\varepsilon^c}{1-c} \quad (39)$$

Eq (39) approaches zero when ε approaches zero. Likewise, when $c = 1$, the Sips isotherm reduced to Langmuir expression. Additionally when $c = 1$, $\sin \pi c = 0$meaning that $N(\varepsilon)$ is zero for all values of ε except $\varepsilon = 0$ where $N(\varepsilon)$ will be equal to infinity. Nevertheless, by substituting in eq(38) and assuming $c = 1$, Sips showed that:

$$\lim_{c \to 1} \frac{1}{RT} \frac{sin\pi c}{\pi} \int_0^{\infty} \left[e^{\varepsilon/RT} - 1\right]^{-c} d\varepsilon = 1 \quad (40)$$

Theoretically, this implies all the active centers on the adsorbent surface have the same energy of the adsorption.

In Figure 9 we show the influence of c value on the distribution of adsorption energies, $N(\varepsilon)$ on the active sites as a function of ε/RT. For $\varepsilon \neq 0$, $N(\varepsilon)$ becomes much smaller when $c = 1$ and it increases to a maximum value when ε is approaching zero (see Figure 9a). When c is near zero (see the figure 9bwhere we showed the $N(\varepsilon)$ for an assumed c value of 0.1 and 0.05), the curve becomes horizontal with linearly decreasing coordinates (more like a Henry type of adsorption).

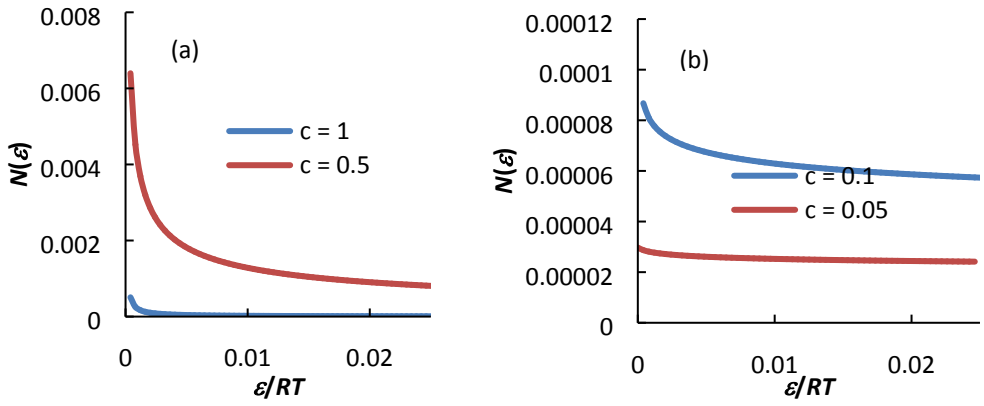

Figure 9(a&b): Site energy distribution according to the Sips isotherm (based on Eq (28)) for different assumed values of c (shown in different panels for convenience).

Sips showed that the method of Stieltjes transform is universal and can be used to extract the theoretical meaning for any empirical adsorption isotherm or any mathematical expression that can represent the experimentally obtained equilibrium adsorption data at a fixed temperature, T. In addition, the Sips isotherm itself is a more generalized mathematical expression and it is possible to propose a large number of mathematical expressions based on the Sips isotherm to represent the experimental adsorption equilibrium data. In fact, a few of the already reported theoretical isotherms can be taken as the limiting cases of Sips isotherm. For instance, the

View Article Online
DOI: 10.1039/C9TA00287A

expression of Hill, which relates the amount adsorbed at equilibrium by the relation given below can still be transformed in to a Sips isotherm. The expression proposed by Hill is:

$$\theta(p) = \left(\frac{p}{p+A}\right)^{c} \quad (41)$$

The Hill expression can be mathematically reduced to the generalized expression of the Sips isotherm by replacing the following terms in Eq (25) as follows:

$\varepsilon = \varepsilon' - b$, $a = A$, $a.\exp(b/RT) = a'$ (42)

Thus, the function that characterizes the distribution of adsorption energies on the binding sites can be written as:

$$N(\varepsilon) = \frac{1}{RT}\frac{\sin \pi c}{\pi}\left[\exp\left(\frac{\varepsilon' - b}{RT}\right) - 1\right]^{-c}, \text{ for } b<\varepsilon \quad (43)$$

As discussed earlier, Sips isotherm reduces to Freundlich isotherm when p is very low ($1 << Ap^c$; see Eq (33)). Provided a new mathematical expression satisfies the condition $0<c<<1$ and if the local adsorption can be represented by a Langmuir expression, then theoretically it is possible to find the corresponding the adsorption site energy distribution function.

Despite the fact that the method proposed by Sips requires several assumptions to characterize the distribution of adsorption energies on the adsorbent surface, it is more straightforward and simpler to use than the discrete method that relies on multi-site Langmuir isotherm expressions. The main limitation of this method is that a reliable site energy distribution function can be obtained only if the isotherm parameters are derived from equilibrium data that covers a wide range of solution concentration or pressure. This method can be properly exploited only if the Sips isotherm constants provide meaningful information based on the experimental equilibrium data that span over a wide range of equilibrium solute concentration. For instance CO_2 molecules will preferentially adsorb on to the functional groups or heteroatoms at low pressure and at higher pressures they progressively adsorb on to the surface that bound micropores followed by mesopores before complete filling of the entire pore volume. [9]Heterogeneity of the CO_2 adsorbents can be characterized using this method only if we have an adsorption equilibrium data that can capture the adsorption in all of the available sites over a wide range of adsorption pressure at equilibrium. Additionally, this method assumes the adsorption isotherm measures only the interactions between the surface and the solute particles. This is essentially true while we deal with adsorption from liquid phase. In the case of gas adsorption the system is more likely to include multi-layered adsorption especially at higher pressures. Additionally, if we deal with subcritical fluid, it is more likely that we encounter a phase change where the adsorption is dictated by fluid-fluid interactions rather than the sorbent-sorbate interaction and such scenarios cannot be precisely captured using this method (this is a general limitation which applies to this method and also for the earlier discussed discrete binding models).

View Article Online
DOI: 10.1039/C9TA00287A

8. Finite difference method

This method was originally developed by Hunston[64] from the basic analytical expression that relates the adsorption of homogeneous solute in solution on to a heterogeneous adsorbent surface given by:

$$q_h = \frac{B}{R_o} = \sum_{j=1}^{m} \frac{n(K_j) K_j F}{1 + K_j F} \quad , \qquad (44)$$

where, $n(K_j)$ is the fraction of adsorption sites with affinity K_j (for each of the *m* class of sites), *B* corresponds to the molar concentration of adsorbed sites, *F* corresponds to the equilibrium concentration of solute in the bulk fluid. R_o is the total concentration of adsorption sites on the adsorbent surface. The total number of sites, n_o is given by:

$$n_o = \sum_{j=1}^{m} n_j \qquad (45)$$

This is essentially the same expression that was used by Scatchard to characterize the protein-ligand interactions (see Eq (1) and Eq (5) discussed earlier). Eq (44) can be applied to characterize the heterogeneity of the material only if we know a value for *m*, which is not known *a priori*. Eq (44) can only be applied if we have information or a reliable assumption on the number of classes of sites, which can be roughly predicted from the Scatchard plot or based on theoretical assumption. Traditionally, a value of 2 is assigned for *m* and a linear regression analysis is performed to obtain the best values for n_j and K_j. For higher values of *m*, an estimation of the affinity parameters and the number of sites becomes extremely complex and also requires user intuition to: decide when to add a new class of binding site; to identify the corresponding *n* and *K* values, and to know when to stop adding a new site classes.

In Figure 10, we show a model distribution or binding affinity spectrum of a polymeric compound that contains three classes of adsorption sites. Assigning the type of sites, *m* = 3 might be a valid assumption for this particular material. However, such assumption might be considered as an overly simplified value especially when dealing with amorphous type activated carbon where one could expect a wide class of binding sites. Even for the polymeric material which is shown in Figure 10, it is theoretically possible to assign a higher value for *m* and draw many tangents to obtain the corresponding *n* and *K* values from each of those tangents. In Figure 10we obtained one such binding affinity spectra assuming *m* > 10. As is shown later, the finite difference method can produce a binding site affinity spectrum which is continuous (rather than discrete) without making any assumptions of the number or type of binding sites.

To overcome the limitation of discrete model, Huston *et al.* replaced the discrete distribution, $n(K_j)$ with a continuous one given by:[65]

$$q_h = \frac{B}{R_o} = \int_{-\infty}^{\infty} \frac{N(K) K F}{1 + K F} d(\log K) \quad . \qquad (46)$$

View Article Online
DOI: 10.1039/C9TA00287A

The total number of sites is given by:

$$n_o = \int_{-\infty}^{\infty} N(K)\log K \quad . \quad (47)$$

The term $\frac{N(K)\log K}{n_o}$ refers togives the probability of finding a site that will have an affinity between $\log K$ and $\log K + d(\log K)$. Theoretically, *N*(*K*) refers to the affinity spectrum, which can be a function of $\log K$ or of *K.* Eq (46)represents only a slight loss of generality and it can essentially capture the discrete spectrum that can be determined using the Scatchard plot or the limiting-slope techniques; the only difference is the spectrum is continuous rather than a series of sharp spikes.

Expressions that are mathematically equivalent to Eq (46) frequently appear in literature and several techniques and methods that include the above discussed method of Stieltjes transform graphical and iterative procedures. All of these methods have several advantages and each have their own limitations. Following the works of Ninomiya and Ferry,[66]Hunston*et al.*[65]used a finite difference method to estimate *N(K)* based on the experimentally obtained equilibrium data. To use the Hunston method, a theoretical or an empirical relation that best represents the experimental equilibrium data (q_h versus the equilibrium solute concentration C_e) is required. Once an appropriate expression is determined, *N*(*K*) can be calculated using the following equation:

$$N(K) = \left| \frac{q_h(aC_e) - q_h(C_e/a)}{2\log a} - \frac{a}{(a-1)^2} \frac{[q_h(a^2C_e) - q_h(C_e/a^2)] - [q_h(aC_e) - q_h(C_e/a)]}{2\log a} \right| \quad (48)$$

In the original work of Hunston *et al.*, to use Eq (48), the experimental equilibrium data is plotted as q_h versus log(C_e) and a trend line that best represent the data is obtained. The best-fit trend line can then be used to extract a value for q_h for a wide range of pressure or concentration. Alternatively, a non-linear regression analysis can be performed to find a theoretical or an empirical expression that best represents the experimental equilibrium data. For example, the equilibrium data can be fitted to a polynomial expression from which we can interpolate the values to get the binding affinity distribution function. This method is straightforward and can instantly produce *N*(*K*) once an expression that closely describes the experimental equilibrium data is known. In Figure 10, we plot the amount of ethyl adenine-9-acetate adsorbed onto a polymer versus equilibrium concentration alongside the theoretically predicted Freundlich isotherm. Also shown in Figure 10bis the binding affinity spectra of this material obtained using Eq (48) based on the equilibrium data obtained using the theoretical Freundlich isotherm (the fitted isotherm is shown in Figure 10a) and assuming $a = 10^{0.2}$. The value of $10^{0.2}$ was recommended by Hunston *et al.,* since it provides the right balance between the spectral resolution and numerical instability. Ideally, a value closer to unity should mathematically mimic the true binding affinity spectrum as $\log a \rightarrow 0$. Hunston earlier showed that such small increments could result in numerical instability. Likewise choosing a larger '*a*' value will lose the resolution of

View Article Online
DOI: 10.1039/C9TA00287A

binding energy spectrum. Thakur *et al.*[67]performed a series of Monte Carlo simulations to obtain the binding affinity spectrum for different cases that consider the influence of surface homogeneity, surface heterogeneity, and different level of random and systematic experimental errors. Their results further confirm that a reliable and a higher resolution spectrum can be obtained for an assumed *a* value of $10^{0.2}$. For comparison we also show the distribution of the binding site constants obtained using the Scatchard plot method (Figure 10b) assuming *m* =3 and *m*> 10. On the other hand, for an assumed value of *m* = 3, we could see only three peaks that characterize the distribution of binding site energy. For the case of *m*> 10, the Scatchard plot produced different binding parameters for the same adsorbent. Eq (48) overcome both of these limitations of the Scatchard plot method and produces continuous and smooth spectra of high resolution capturing the affinity parameter of the binding sites available on the adsorbent surface over a wide range of solution concentrations. Additionally, the binding affinity obtained with Eq (48) seems to be comparable with those obtained using Scatchard plot method. This instantly shows how this numerical method can produce reliable binding affinity (with values comparable to the one obtained with discrete method) spectra without requiring any prior information on the number or the type of binding sites or user intuition.

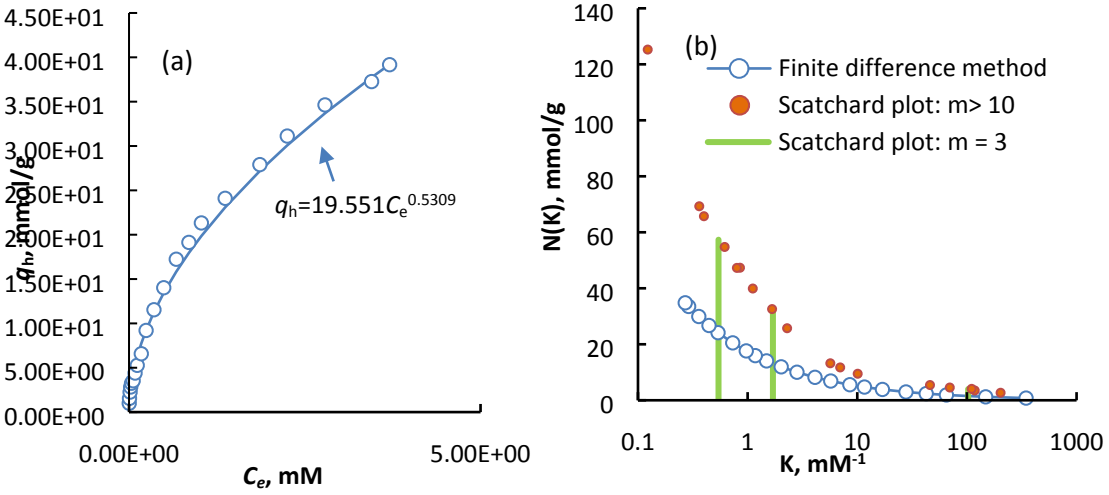

Figure 10: (a) adsorption isotherm of ethyl adenine-9-acetate adsorbed onto a polymer (experimental data taken from the works of Umpleby*et al.*[68]) ; (b) adsorption site energy distribution predicted using Scatchard plot method and the finite difference method.

Similar to the previously discussed condensation approximation method, Eq (48) can also be used to estimate the characteristic energetic distribution of any theoretical isotherm. This can be readily achieved by simply replacing the q_h values in Eq (48) with the corresponding theoretical isotherm. For instance, the site energy distribution function or the theoretical ideas that dictates the characteristic properties of Sips isotherm can be obtained by substituting Eq (33) into the Hunston equation. In Figure 11, we show the site affinity distribution spectra of several hypothetical adsorbents that have a maximum adsorption capacity of 30.8 (a.u) but different level of site heterogeneity and binding affinity. For *n* = 1, according to Eq (48) the Sips isotherm exhibits a quasi-Gaussian distribution of binding site energies. It should be remembered that according to

View Article Online
DOI: 10.1039/C9TA00287A

the method of Stieltjes transform, this isotherm exhibits a Gaussian energy distribution. Nevertheless Eq (48) retains the theoretical essence of the Sips isotherm. For lower values of *n*, the Sips isotherm exhibits a more exponential distribution of site energies especially at lower concentrations. Another noteworthy point is that the mean energy (for fixed values of *b* and q_m) is not significantly influenced by *n* value. The higher the Sips isotherm constant, *b*, the narrower the site energy distribution, and in this case adsorption sites host solute molecules only at higher concentration or pressure. For lower values of *b* and *n*, the adsorption energies are exponentially distributed. Figure 11 thus shows how the simple analytical expression (Eq 48) obtained by Hunston *et al.* can be used to bring theoretical insights on theoretical adsorption like Sips isotherm. Obviously, any expression can be substituted for the *q* value and their theoretical concepts can be explored. In fact, even a new empirical expression can be proposed and its theoretical justification, if any, can be deduced using this expression.

To demonstrate this method, in Figure 11c, we show the site affinity spectra of the most frequently used Redlich-Peterson (RP) isotherm. The RP isotherm is given by:

$$q = \frac{Ap}{1 + Bp^g} \quad , \qquad (49)$$

where, *A* and *B* are isotherm constants and are related to the adsorption capacity and binding energy, and *g* is the isotherm constant related to the heterogeneity of the adsorbent. When *g* = 1, Eq (49) transforms into a Langmuir isotherm. At higher pressure, this expression becomes a Freundlich isotherm:

$$q = \frac{A}{B} p^{1-g} \quad . \qquad (50)$$

The site energy spectra should predict both of the above scenarios. In Figure 11c we tested this by obtaining the site energy distribution spectra of the RP isotherm using the finite difference method. The site affinity spectra were generated by assuming different values of the isotherm constants *B* and *g* and for a fixed value of adsorption capacity, *A* = 30.8. When *g* = 1, the RP isotherm exhibits a quasi-Gaussian distribution of binding site affinities (or energies). This means the RP isotherm represents a more homogeneous adsorption when *g* = 1. For *g*< 1, the RP isotherm exhibits a more heterogeneous site distribution and the adsorption site energies are exponentially distributed. The lower the RP isotherm constant, *B* the narrower the site energy distribution with most of the adsorption sites hosting solute molecules only at higher concentration or pressure. Decreasing the *g* value progressively shifts the site affinity spectra from a quasi-Gaussian to an exponential trend. This means that for lower *g* values, this isotherm follows a Freundlich type of isotherm and when *g* = 1, this isotherm represents a more homogeneous surface or in other words a Langmuir type of adsorption isotherm. Another notable feature is that when *b* = 1 and *g*= 0.8, this isotherm represents the combination of the two distributions; an exponential distribution of low affinity binding sites and a quasi-Gaussian distribution of higher affinity binding sites. This means for a specific value of *g* and *b*, this isotherm can capture the both heterogeneous and homogeneous surface adsorption properties. For

View Article Online
DOI: 10.1039/C9TA00287A

example, such a theoretical scenario can be realized experimentally during the adsorption of small molecules like CO_2, N_2, H_2, CH_4 onto highly microporous and functionalized carbon materials. The molecules will be adsorbed first on to high affinity binding sites at lower pressures after which the gas molecules will adsorb in the uniform sized micropores where one could expect a more homogeneous adsorption. This result can be tested by fitting the experimental equilibrium data in RP isotherm and the fitted isotherm parameters can be later substituted in Eq (49) to obtain the corresponding site affinity spectrum. For the convenience of the readers, as a supplementary file we uploaded the Microsoft excel spreadsheet where we explained in detail how to get the site energy distribution spectra using the numerical method discussed in this section.

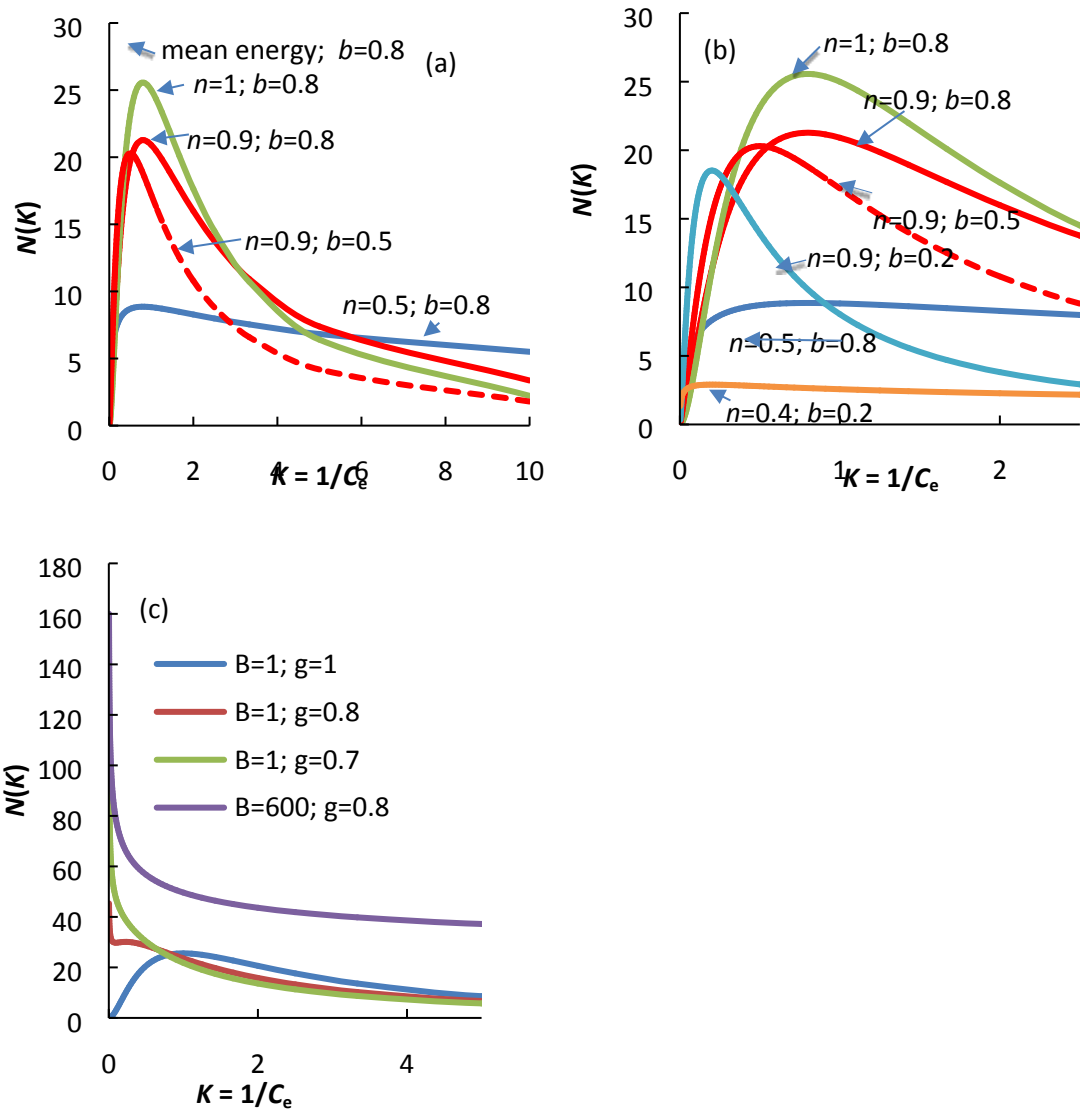

Figure 11: (a-b) Influence of the Sips isotherm constants (*n* and *b*) on the site energy distribution spectra for a fixed adsorption capacity, q_m= 30.8 and for a combination of Sips isotherm constants. Figure a, we show the mean energy of the adsorption sites is constant for a fixed value of *b* = 0.8; Figure b is shown only for clarity purpose and to emphasize the shift in mean energy as a function the Sips isotherm constant *b*); (c) Influence of the Redlich-Peterson isotherm constants on the

View Article Online
DOI: 10.1039/C9TA00287A

adsorption site energy distribution spectra; the maximum adsorption capacity was fixed to A = 30.8.

The numerical method is useful particularly when dealing with isotherms that involve several isotherm constants. For instance the Dual-Site-Langmuir-Freundlich isotherm (DSLF) (Eq (51)) is most widely used by the material scientists mostly to model the adsorption equilibrium data of several small gas molecules by different porous materials. [69–71]

$$q = q_{m1}\left[\frac{b_1 p^{n_1}}{1+(b_1 p)^{n_1}}\right] + q_{m2}\left[\frac{b_2 p^{n_2}}{1+(b_2 p)^{n_2}}\right] \quad (51)$$

The presence of multiple isotherm constants (up to six constants) provides mostly the best-fit for the experimental data. For instance, this particular isotherm involves six isotherm constants. The six isotherm constants, b_1, b_2, n_1, n_2, q_{m1} and q_{m2} can be easily obtained using a simple non-linear regression analysis my minimizing an appropriate error function that measures the difference between the experimental equilibrium data and the predicted DSLF isotherm. Once the adsorption isotherm constants are predicted, the binding site affinity function, $N(K)$ can be determined from Eq (48) using the above explained protocol. Applying Eq (51) in Eq (48) should essentially yield a quasi-Gaussian distribution spectra similar to the ones obtained earlier using Eq (22). For the convenience of the readers, in the supplementary file a Microsoft spreadsheet is provided which explains the ways to obtain $N(K)$ using the numerical technique discussed in this section from the two widely used adsorption isotherms, Langmuir-Freundlich isotherm and the Freundlich isotherm. This protocol can be extended to any theoretical adsorption isotherms; the only difference is that the q_h in Eq (48) will be replaced by a suitable theoretical adsorption isotherm.

Irrespective of the theoretical isotherm used, as in the condensation approximation method, the accuracy of the affinity spectrum can be regulated by controlling the analytical window where one could expect more meaningful information about the binding site affinities. Similar to the condensation approximation method, the binding affinity window can be determined from the minimum and maximum pressure or equilibrium concentration in the bulk phase in the experimental adsorption isotherm:

$$K_{min} = 1/C_{e,max} \& K_{max} = 1/C_{e,min} \quad (52)$$

9. Expectation-Maximization method

Stanley and Guiochon suggested the application of an Expectation-Maximization (EM) algorithm as a robust method to obtain the site energy distribution function from the inverse equation of the fundamental equation of the adsorption of heterogeneous surfaces.[72] This method does not require any prior knowledge of the adsorption isotherm model describing the overall adsorption data, nor any smoothing of the experimental data. The EM method is applied directly to the raw experimental data and therefore involves a low amount of artifactual information from a numerical standpoint, and so provides a relatively unbiased solution. Additionally this method does not require any prior information about the error distribution.

View Article Online
DOI: 10.1039/C9TA00287A

According to the method, the site energy distribution function, $F(E)$ is characterized using a grid of N points in the energy space between E_{min} and E_{max}; i.e., the energy space is represented by NE_i grid points. Likewise, the concentration range (from experiment) is also discretized using a grid of M points in the concentration between p_{min} and p_{max}; i.e., the pressure space is represented by Mp_j points. The amount $q(p_j)$ at concentration p_j is iteratively determined. At the k_{th} step of the iteration process, the amount adsorbed is given by:[72]

$$q^k_{calculated}(p_j) = \sum_{i=1}^{i=N} F^k(E_i)\theta(E_i p_j)\Delta E;\ j \in [1, M];\ i \in [1,N] \quad , \quad (53)$$

WhereΔE is the grid spacing around each energy point i and the sum is over the concentration points$j$. ΔE and E_i are defined by the following equations:

$$\Delta E = \frac{E_{max} - E_{min}}{N-1} \quad , \quad (54)$$

$$E_i = E_{min} + (i-1)\Delta E \quad . \quad (55)$$

The site energy distribution function at the k_{th} iteration is then updated using the following equation:

$$F^{k+1} = F^k(E_i)\sum_{j=1}^{j=M} \theta(E_i p_j)\Delta E \frac{q_{experimental}(p)}{q^k_{calculated}(p_j)} \quad , \quad (56)$$

where, $q_{experimental}(p_j)$ is the experimental isotherm data and $q^k_{calculated}(p_j)$ is the estimated isotherm at iteration k using equation (56).

The use of the above equation requires a set of initial estimation of $F(E_i)$ as the method maximizes the influence of data over the final distribution. The initial guess used to determine the site energy distribution function is based on the 'total ignorance' guess:[72–74]

$$F^o(E_i) = \frac{q_{experimental}(C_{maximum})}{N} \quad (57)$$

This means the initial distribution is constant for all the sites 'i'. The iterations are performed beginning with M, N, E_{max}, E_{min}, C_{max} to obtain the site energy distribution function and the final result is a distribution of equilibrium constants. The iteration procedure continues until the sequence monotonically converges to the more probable estimation that the data follow either Gaussian or Poison distributions. This method has its own advantages; mainly it relies on the iterative procedure and does not require any unrealistic assumptions. On the other hand, coding is required to solve the site energy distribution function, so this method cannot be performed using a simple analytical calculation in order to obtain the affinity distribution spectra. The main advantage of this method is that it has been validated experimentally. This method successfully predicted the site energy distribution of porous silica and its C-18 bonded derivative, molecularly imprinted polymers for a wide range of molecular probes.[7572,7673]Specifically, this method was able to reveal the heterogeneity of molecularly imprinted polymers. Recently, the method was successfully used for protein-ligand screening.[74] With sufficient number of iterations, this method can unambiguously discriminate different types of adsorption sites having energy difference of less than 4-5 kJ/mol.[75]The main limitation of this method is that it cannot distinguish between the adsorption sites having energies less than 2 kJ/mol.[75] Another limitation is that this method produces reliable adsorption energy distributions only when majority of the adsorption energy is approximately 10 kJ/mol greater than the solute's heat of vaporization, and only when solute-solute interactions are not significant when compared to its adsorption energy.[75] A careful

View Article Online
DOI: 10.1039/C9TA00287A

analysis of the literature shows, that though this method is widely accepted, its use is limited and most of the works comes from a specific research group and mostly to characterize molecularly imprinted polymers. Another limitation is that the implementation of the method requires sophisticated coding to tailor its use fora specific physical system. Such coding skills are not typical for many experimental materials chemists, which perhaps explain why the use of this powerful method is largely limited to one specialist research group.

10. General comments, common limitations of the binding site energy spectra

All the theoretical approximations, empirical and the numerical methods discussed in this review can mostly be applied to Type 1 adsorption isotherms on microporous materials. This means, all of these discussed methods can be used wherever Type I isotherms are encountered. For example, these methods can be used to characterize the materials for the binding site energy heterogeneity based on the equilibrium obtained for (i) small gas molecules on to any porous materials,[77,78] (ii) adsorption of several targeted materials from their aqueous solutions,[79] (iii) characterization of any new functional and porous materials based on their N_2/CO_2 adsorption isotherms,[80] (iv) protein-ligand binding interactions,[81] (v) gas sensing materials,[82] (vi) ion-exchange materials,[83] (vii) packing materials in chromatographic columns,[84] etc.

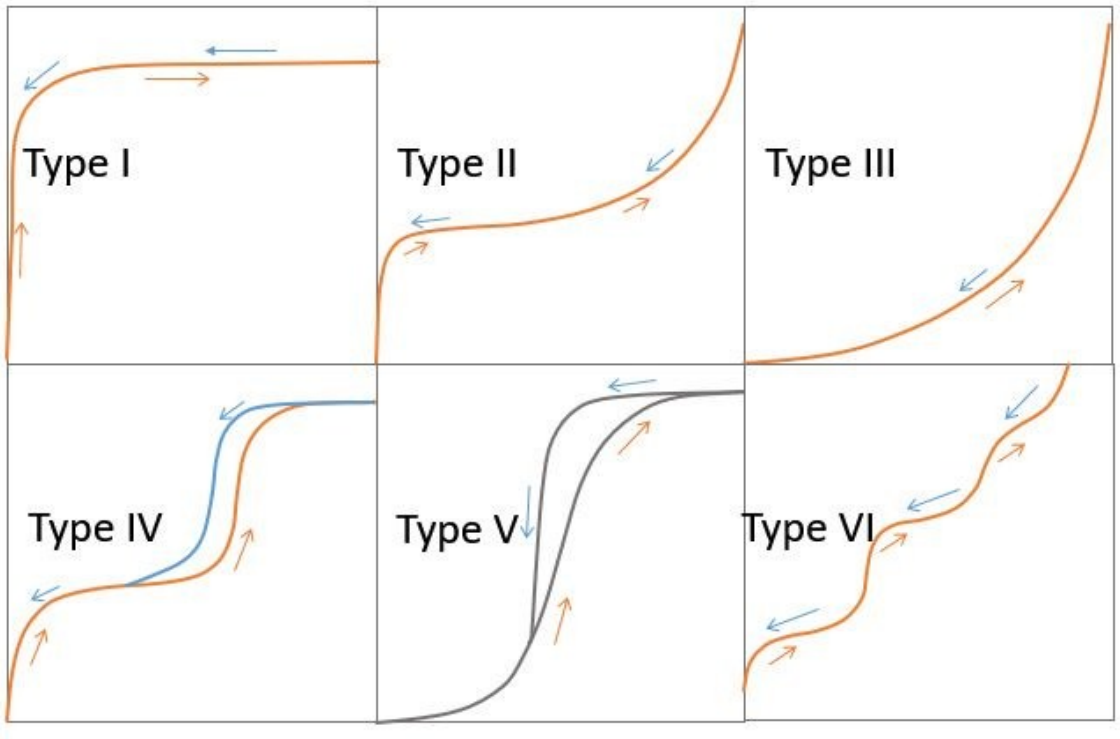

Figure 12: Different types of adsorption isotherms as classified by IUPAC.[25]

Care must be taken, as these methods cannot be easily applied or transformed while dealing with the Type II, Type III, Type IV, Type V and Type VI isotherms as classified by IUPAC (see Figure 12).[25] The other type of isotherms such as Type II to IV normally indicate the coexistence of sorbate-sorbate interactions and also vary the respective contributions with the each Type of isotherm.

View Article Online
DOI: 10.1039/C9TA00287A

Thus isotherms of other than Type I are more complex in nature to obtain information about the surface heterogeneity For example, the Type II to IV isotherms are mostly observed in the hierarchical porous solids of wide range of pore-size distribution spanning across micro-meso-and macro-pore regime, and where the pertaining porosity in each region vary significantly. For instance, in the Type-II isotherms of the combined micro-/mesoporous adsorbents the forces involved are due to the combination of the adsorbent-adsorbate and adsorbate-adsorbate interactions. In such cases, to extract information about the heterogeneity of the adsorbents simply from the adsorption isotherms is a complex task. Therefore alternative methods that can reveal the distribution of the active sites in such surfaces are necessary. One way to analyse such materials is to obtain the site energy distribution spectra based on the measured adsorption isotherm at relatively lower pressure region, before the actual pore-filling effect region, using commonly utilized adsorption isotherms like Toth, Freundlich and Sips isotherms. This typically corresponds to the adsorbate-adsorbent interactions.

Type III isotherms are a typical example, where adsorbate-adsorbate interactions dominate and in that case a simple estimation of isosteric heat or information about the density of the fluid inside the pores as a function of pressure will give information about the type of energies involved in the sorption process. In this case the energies involved will be mostly equivalent to the energy of liquefaction. Another peculiar case is the Type V isotherm, where again adsorbate-adsorbate interactions dominate, and purely adsorbent-adsorbate interactions are barely observed. In this case, it would be a difficult task to apply any of the above methods discussed. These are the common limitations of the above methods, as the site energy distribution functions are mostly proposed in literature to characterize materials with functionalities that can be titrated using simple gas adsorption or liquid adsorption equilibrium data. Type VI isotherms that have several steps in the adsorption isotherm due to the representative layer-by-layer adsorption are also difficult to treat with the methods reviewed in this work. One possibility is to fit the first adsorption step that can be observed in the experimentally obtained adsorption isotherm in a suitable theoretical adsorption model. Typically, this zone should essentially capture the adsorbent-adsorbate interactions especially at lower partial pressures. The determined isotherm parameters can later be used to determine the site energy spectra using the condensation approximation method detailed in the Section 6.

In other peculiar cases, as in water adsorption, it is common to expect secondary events like cluster formation, co-adsorption, creation of new active sites due to the adsorbed water molecules.[21,85,86] Obviously, such information cannot represent the actual heterogeneity of the material. So clearly for this case, the proposed methods should not be applied. It is also worth mentioning here about the recently appearing flexible or soft porous crystals or flexible MOFs whose pore volume and surface chemistry are sensitive to pressure.[87,88] The physics involved in such materials is in an emerging state and is still not definitively understood. Also, flexible porous materials lack the actual adsorption zone and the pore-widths are changed upon guest molecular adsorption/desorption. This change is also largely depending on the type of adsorbate and sorption conditions. The best example of the material is a special category of MOFs, called MIL-53. These structures porosity and unit cell volume change considerably upon guest insertion/removal and also strongly depend on the molecule type –such as structures show very

View Article Online
DOI: 10.1039/C9TA00287A

different adsorption isotherms for H_2, N_2, CH_4, CO_2, H_2O or other hydrocarbons.[89] Such behavior is not normally observed in rigid porous solids.

Additionally, all such materials lack the adsorption zone which is dominated by purely adsorbent-adsorbate interactions and the empirical, numerical approximations discussed in this review may be too simplistic to quantify the adsorption site energies involved in such materials. Clearly such materials can only be modeled using rigorous computational modeling at molecular level, based on the isosteric heat as a function of loading, the number and type of adsorption sites and their binding energies can be estimated.[90]

11. Isosteric heat

It has been long realized that the differential heat of adsorption, Δh, that corresponds to the heat evolved during the physical adsorption of gases on solids will provide the information about the nature of the solid surface.[91,92] The amount of heat evolved when a certain amount of gas is bought in to an adsorbed state at a fixed pressure p and temperature T depends on the binding energy of the active sites and the number of the binding sites available on the surface. Typically, this corresponds to a value when one equilibrium condition transitions to another equilibrium condition. This makes Δh different from the integral heat of adsorption, which always corresponds to the heat of liquefaction i.e. the amount of heat evolved when a gas is brought into contact with the minimum amount of adsorbent to uptake the gas.[93]Alternatively, Δh can be defined as the energy necessary to remove an adsorbed molecule from its average vibrational state and from the attractive forces of its adsorbed neighbors to an infinite distance from the surface, plus the energy equivalent to the degrees of freedom of the molecules of the gas in excess of those in the adsorbed state. Calorimetric experiments can provide information about the differential heat of adsorption. Instead, precise information about the heat of adsorption itself can be obtained from adsorption isosteres. A plot of the variation of the equilibrium pressure with temperature corresponding to a constant amount of gas adsorbed, is called an adsorption isotere.[94] Isosteres resembles the vapor pressure curves of liquids; pressure increases slowly with temperature at first followed by a rapid increase with temperature. In a vapor pressure curve, every point represents the equilibrium condition between a vapor and its liquid at a particular pressure and temperature. In the case of isosteres, every point represents a pressure and temperature at which the adsorbent-adsorbates in equilibrium with the bulk fluid. Mathematically, the isosteric heat, q_{st} is defined as the differential enthalpy with reversed sign and is obtained from the Clausius-Clapeyron equation:[95]

$$\left(\frac{\partial \ln p}{\partial T}\right)_q = -\frac{\overline{h_a} - h_g}{RT^2} = -\frac{\overline{\Delta h}}{RT^2} = \frac{q_{st}}{RT^2} \qquad (58)$$

Where, q_{st} can be the total number of moles adsorbed per unit area at pressure p and temperature T, h_a is the mean molar enthalpy of the adsorbed molecules, h_g is the mean molar enthalpy of gas and Δh is the differential enthalpy of adsorption. The above equation is widely accepted to obtain the q_{st} in order to understand the nature of adsorption or for material screening. Typically, a plot of ln p versus $1/T$ at constant surface coverage should produce a straight line with a slope equal

View Article Online
DOI: 10.1039/C9TA00287A

to $-\overline{\Delta h/R}$. The slope will be equivalent to isosteric heat of adsorption and this value typically reaches heat of vaporization when the gas molecules are completely condensed inside the adsorbent pores.

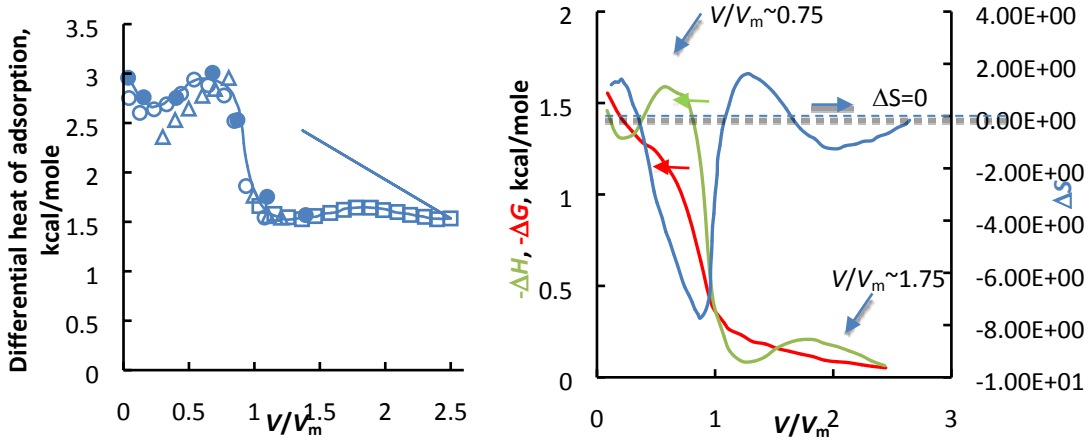

Figure 13: (a) Calorimetrically determined differential heats of adsorption for N_2 as measured by Beebe et al., [96] (shown as open and filled blue circles) and determined isosterically by Joyner and Emmett (open blue squares: 68.3 K – 90.2 K, solid blue lines: 78.2 K – 90.2 K, open blue triangle: 68.3 K – 90.2 K); (b) Graph showing the variation in the free energy change, change in the adsorption heat and the change in entropy as obtained by Joyner and Emmett (see the discussion in this text).

The isosteres are usually obtained at constant amount of adsorption or surface coverage. Alternatively, isosteric heat can also be obtained at a constant volume of adsorbed gas at several studied temperatures. In the year 1938, Wilkins in his classical paper recommended obtaining isosteres at constant fraction of surface coverage.[97] Later in 1942, Joyner and Emmett experimentally showed that it is more accurate to obtain adsorption isosteres at constant volume of adsorbed gas rather than at a constant surface coverage.[98] They also showed, isosteres obtained based on constant surface coverage resulted in lower q_{st} values compared to the ones obtained with constant volume of adsorption; the difference is ~ 100 – 400 calories for the adsorption of N_2 gas on carbon blacks. Additionally Joyner and Emmett for the first time showed that the isosteres obtained based on constant volume of adsorption matched the heat of adsorption obtained from calorimetric experiments, by Beebe *et al*[99] for the same system with remarkable accuracy.

Alternatively the adsorption equilibrium data obtained at two different temperatures can be used to get the q_{st} value, the following linearized form of Clausius-Clapeyron equation can be used:

$$-q_{st} = \Delta H = 2.303R\left(\frac{T_1T_2}{T_2 - T_1}\right)\left[log\ p_2 - log\ p_1\right]_{at\ constant\ q} \quad (59)$$

View Article Online
DOI: 10.1039/C9TA00287A

In this case, for each isotherm, log p can be plotted against the volume of gas adsorbed. The vertical distance between the lines can then be measured at a given values of q and inserted in to the Eq (59) to obtain the isosteric heat. If the adsorption isotherms are obtained at more than two different temperatures, Eq (59) can be used to obtain isosteres in more than one way. The vertical lines can be drawn between any of two lines (log p_2-log p_1 or log p_3-log p_1 or log p_2-log p_3) in order to obtain the isosteres and can be compared against each other (This is shown in Figure 13(a)). Joyner and Emmett further successfully demonstrated that Eq (59) produced the unusual calorimetric curve observed for the adsorption of N_2 on graphon. Adsorption isotherms at three different temperatures, 90.2 K, 78.2 K and 68.3 K used to obtain the isosteric heat using Eq (59) in three different ways using three different pair of the isotherms. In Figure 13a, we reconstructed the isosteric heat obtained by Joyner and Emmett for N_2 adsorbed on to carbon black, graphon. They found that for monolayer coverage above 0.7 the isosteric heat produced by any two pair of isotherms matches with the ones obtained from adsorption calorimetry. The isosteric heat obtained below 0.7 monolayer coverage slightly deviates from the calorimetric values and attributed this discrepancy to the error associated with the adsorption experiments at 68.3 K due to the low absolute pressure involved. This also explains why the heat values calculated from the pair of the isotherm obtained at 68.3 K and 90.2 K are in poor agreement with the calorimetric values. Their results also demonstrate how accurate adsorption energies can be obtained from isotherms by controlling the experimental conditions. This work still remains one of the seminal adsorption papers. In fact, the works of Joyner and Emmett pointed out the presence of the surprisingly feature of two humps in the isosteric heat separated exactly by one monolayer of the N_2 molecule. The first hump is at ~0.75 (shown by arrows in Figure 13(b)) and the second one at ~1.75 (see Figure 13(b)), though the later one is not a steep rise as compared to the first one. They proposed the concept that whatever the forces are involved in the first rise are carried through and repeated in the second layer. One way to find an explanation for this type of behavior is to obtain other thermodynamic parameters, for example, from the calculated heat of adsorption.

The calculated isosteric heat can also be used to obtain some fundamental information about the way the molecules are assembled in the pores. Joyner and Emmett showed this by obtaining the thermodynamic parameters, ΔH, ΔG and ΔS for the sorption of nitrogen on Graphon.[100] Literature show multiple ways to obtain these thermodynamic parameters. Here we describe the way Joyner and Emmett method. For a simple process where a phase change is involved, say for example from gaseous N_2 to liquid and adsorbed N_2. The free energy change ΔG can be obtained from the expression:

$$\Delta G = RT\ ln\left(\frac{p}{p_0}\right) \quad . \quad (60)$$

For $0/p_o < 0$, the process will be spontaneous; for $p = p_o$, the system will attain equilibrium, and for $p > p_o$, adsorption will cease.

Based on the determined ΔH (from Eq (59)) and ΔG values, the entropy change, ΔS as a function of the amount adsorbed can be determined from the relation:

$$T\Delta S = \Delta H - \Delta G \quad . \quad (61)$$

View Article Online
DOI: 10.1039/C9TA00287A

Joyner and Emmett obtained the change in entropy as a function of surface coverage for the adsorption of N_2 on Graphon: we showed their determined values in Figure 13(b).[100] They provided theoretical justification for the unusual humps observed in the isosteric heat (see Figure 13(a)) based on the entropy value (in Figure 13(b)). They observed ΔS remains positive up to a V/V_m value equal to 0.3 and again for a V/V_m value between 1.0 to 1.5 (Figure 13(b)). They attributed the negative entropy change during the adsorption to the ordered arrangement of adsorbed molecules on the active sites. The small positive portion of the entropy curve for V/V_m< 0.3 was assumed to be due to the disordered arrangement of adsorbed molecules. Once the surfaces are partially covered, then the molecules tend to adsorb in a more ordered way which should be reflected by a negative entropy change. Bebe and his co-workers interpreted this behaviour as adsorption region where the interactions between adsorbed molecules are negligible.[96] Joyner and Emmett mentioned the observed increase in entropy and also the ΔH for V/V_m between 1.0 -1.5 may not be due to the disordered arrangement of molecules in the second adsorbed layer (Figure 13(b)). However, all of these possibilities and theoretical interpretations made by Joyner and Emmett and in the works of Beebe *et al.* are theoretically correct.

In the last few years, several theoretical studies performed using molecular level simulations to understand the random arrangement of the adsorbed species in the functional or defective heterogeneous surfaces or due to the confinement. Kumar *et al* showed the adsorbed CO_2molecules are slightly tilted from the surface of N doped carbons.[9] It was also observed that CO_2 molecules lie parallel to the pore surface. Molecular simulations also showed that fractional layers of gas molecules (for example 1.5, 2.5 and 3.5 layers) in the pores tend to pack in a more disordered manner as the molecule adsorbed on one side of pore effect the adsorption on other side of the pore-wall. Gotzias *et al*[101]performed molecular simulations to study the adsorption of Ar at 87 K in pristine and oxygen functionalized carbons. It was found that the isosteric heat due to solid-fluid interactions decreased with surface coverage whereas the isosteric heat due to fluid-fluid interactions progressively increased, especially at higher loadings. Both observations match the interpretation of Joyner and Emmett: an increase in ΔH is due to domination of fluid-fluid interactions, and a decrease in ΔH indicates the heterogeneous nature of the adsorbent.

Another method which has recently been getting attention is to obtain the isosteric heat from virial type expression.[102] Virial expression is more flexible and the number of isotherm constants involved can be chosen until this expression precisely fits the experimental equilibrium data. This was mostly used to model the isotherms of zeolitic fluids.[103] This expression relies on the assumption that independent of the nature of the sorption process, it can relate the intra-crystalline concentration and the mean hydrostatic stress intensity or osmotic pressure. The virial isotherm is given by [104]

$$K = \frac{a_s}{a_g} = \frac{q}{p} e^{\left(2A_1 q + {}^{3}/_{2} A_2 q^2 + \ldots\right)} \qquad (62)$$

Where, K is the thermodynamic equilibrium constant for the distribution of the sorbate between the gas phase and the sorbate-sorbent mixture or also the Henry's constant, a_s is the equilibrium activity of the sorbate in the solid and a_g is the equilibrium activities of the sorbate in the bulk gas, n is the concentration of the sorbate in the sorbate-sorbent mixture over which the

View Article Online
DOI: 10.1039/C9TA00287A

equilibrium pressure is p. A_1 and A_2 are the virial coefficients which depend on the temperature and nature of the sorbate and sorbent and is independent of the concentration, q. A simple non-linear regression analysis can be used to predict the virial isotherm constants from the experimental equilibrium data (please see the supplementary information where the method to obtain the virial coefficients and the Henry's constant from a model equilibrium data set is shown in a Microsoft Excel spreadsheet).

Another type of Virial equation in the exponential form, as used by Bradley[105,106] and Wilkins[97], is given by

$$p = qe^{(C_1 + C_2 q + C_3 q^2 + \ldots)} \quad (63)$$

Where C_1, C_2, C_3 are the virial isotherm constants and often refer to the primary adsorbent-adsorbate interactions, double and triple interactions in the adsorbent field and these values include the possible effect of inhomogeneity in the surface. In Eq (62) and Eq (63), typically up to four coefficients can describe a considerable region of the coverage. [106]

According to Eq (62), the Henry's constant, K can be found by simply extrapolating the plot of ln(p/q) versus q according to the expression.[103,104]

$$ln\left(\frac{p}{q}\right) = ln\left({}^{1}/_{K}\right) + 2A_1 q \quad (64)$$

According to the above expression, a plot of ln(p/q) versus q should be linear at concentrations well above the Henry's law limit. Only then will the extrapolation of the plot to zero q provide a reliable Henry's constant. The K value can be directly used to screen the porous materials for their selectivity towards a specific molecule. The K value can be used to obtain the adsorption heat using the Clausius-Clapeyron expression:[103]

$$\Delta H = RT^2 {}^{d(ln(K))}/_{dT} \quad (65)$$

It must be mentioned that the K value measures the binding forces involved at zero coverage, so it can provide information about the selectivity of an adsorbent for a specific target molecule based on the adsorption forces involved purely between solute-sorbent, where sorbate-sorbate interactions are negligible. The values obtained from the above expression (Eq (65)) should estimate the adsorption isosteric heat at zero coverage. Such values are often useful in screening porous materials for their gas sensing properties and selectivity in the case of adsorption in fluid mixtures. Alternatively, the determined Henry's constant and the virial isotherm constants obtained from Eq (63) at two different temperatures can be used to determine the isosteric heat using Eq (59).

Another frequently used Virial expression is given by:

$$\ln p = \ln q + \frac{1}{T}\sum_{i=0}^{m} A_i q^i + \sum_{i=0}^{n} B_i q^i \quad (66)$$

Where A_i and B_i are the virial isotherm constants.

The above expression was proposed assuming Q_{st} is independent of temperature within a limited range of temperature. Eq (66) seems to successfully represent the experimental equilibrium data with a high level of accuracy using relatively low polynomial orders and that usually $n < m$. The virial isotherm constants can be easily obtained using a regression analysis where a suitable error function can be used to minimize the error distribution between the experimental data and the isotherm predicted by Eq (66). The determined virial coefficients can

View Article Online
DOI: 10.1039/C9TA00287A

be used to obtain the isosteric heat as a function of loading by applying the Clausius-Claypeyron expression. Substituting Eq (66) in Eq (58) should give

$$q_{st} = -R\sum_{i=0}^{m} A_i N^i \quad (67)$$

Isosteric heat of adsorption is an important parameter and can give information about the heterogeneity of the adsorbent. Clearly the isoteric heat of adsorption can complement the site energy distribution spectra obtained from the methods discussed in the previous sections. To obtain reliable information about the isosteric heat it is essential to obtain experimental adsorption isotherms at least two different temperatures. Alternatively, the site energy distribution function can bring similar information especially about the heterogeneity and how the adsorption site energies are distributed just from an adsorption isotherm obtained at one temperature. Additionally, site energy distribution spectra can provide information about the nature of adsorption and the type of adsorption sites that are occupied as a function of temperature. For example, it is possible to obtain information about the nature of adsorption for a specific material from the site energy distribution based on the adsorption isotherms obtained at two different temperatures, for example one at cryogenic conditions and another one at room temperature. This is not practically possible with isosteric heat as Eq (59) described can be applied successfully only when the adsorption isotherms are obtained at temperatures that are not more than 5 ^{o}C from each other. Obviously, it is possible to rely on both isosteric heat and the site energy distribution models/methods discussed here, and both can be used as they will complement each other and bring new insights about the physics involved during the adsorption.

12. Fontal affinity chromatography

Competition effects are often encountered during the multi-component adsorption of solute molecules from their mixtures. The adsorption site energy distribution can provide useful information about what type of sites are occupied by a specific target molecule from a fluid mixture. Alternatively, it can also give information about what type of adsorption sites are occupied by the competing molecules. The site energy distribution can provide information about whether high energy binding sites or the low energy binding sites are occupied from the competing sites. Such information can be obtained provided the experimental set-up permits the simultaneous study of the adsorption equilibrium of a single component from the multi-component system. Examples include, adsorption of CO_2 plus CH_4, a commonly encountered fluid mixture in coal bed methane recovery, and the adsorption of CH_4 plus H_2, a common mixture also called as hythane that can be used as an alternate fuel to gasoline.[20,107] In H_2 purification, the separation of CO_2 from H_2 is other issue.[108] Mixtures of different solute molecules are also often encountered during the purification of wastewater treatment, chromatographic separations, in life science to determine the specific interactions between biomolecules, drug-protein interactions, etc.[109,110,111] If one has the information about the single component adsorption isotherm and the multi-component adsorption isotherms, then it is possible to determine what type of adsorption sites are occupied by each of the components during the adsorption from fluid

View Article Online
DOI: 10.1039/C9TA00287A

mixtures. Frontal Affinity Chromatography (FAC) is a useful technique and allows obtaining such information experimentally.

Depending on the adsorption capacity of an adsorbent for different fluids in a mixture at least three different case scenarios can be encountered: (i) all the components have the same level of adsorption strength and the adsorption capacity of components is independent of each other; i.e., they follow the Henry's law, adsorption increases linearly with concentration, (ii) each of the components in the mixture possess different sorbabilities on the adsorbent but follow the Henry's law and (iii) all the components in the mixture possess different level of sorbability and compete with each other for the same site on the adsorbent or in other words the sorption of one component depends on the concentration of the other component.

For the *case 1*, the adsorption of the mixture components can be same as that of adsorption of their single components. In this case, irrespective of the composition, the adsorption can be just the function of initial concentration of each component. This frequently occurs when the adsorbent surface contains templated pores that can hold only a specific type of molecule. For instance, in molecularly imprinted polymers, the efficiency of the templating synthesis techniques and how many of the template molecules are removed from the adsorbent framework template, can be tested by adsorbing a fluid mixture that contains the template molecule and an external molecule that may be indifferent to that of the template molecule in terms of size and shape.

Case 2 is also a special case of case 1, the only difference being that the number of binding sites available for the uptake of each component in the mixture is different. For instance, the same adsorbent can uptake more amount of component 1 than component 2 however, the adsorption capacity of respective components is not affected by the actual composition the mixture.

Case 3 is complex and the most commonly encountered phenomenon on different classes of adsorbents. Simple adsorption experiments performed at batch scale can provide information about the adsorption capacity; though it cannot give information about how the composition of each of the adsorbates in their mixture affects the adsorption capacity of the adsorbents.

FAC is a versatile and powerful technique to characterize adsorbents for their affinity for specific type molecule or more than one type of molecules, and also to understand the influence of the concentration of these. FAC can be used to obtain equilibirium data and information about the adsorption mechanisms involved in all the three cases discussed above. This technique was originally developed by Tiselius and Claesson, mostly to study the adsorption of targeted molecules from a single or a binary mixture.[112,113] The concept is simple and similar to the batch adsorption experiments. The equilibrium adsorption capacity of an adsorbent for single or multicomponent is experimentally obtained at different concentrations; the only difference is that the same experiment is performed in a column filled with adsorbent in a semi-continuous mode. In FAC, the titration of active sites of the adsorbent is performed by passing the adsorbate of known concentration in a carrier uninterruptedly through the column. As the adsorbate flows through the column, it adsorbs to and saturates the active sites and the adsorbate concentration

View Article Online
DOI: 10.1039/C9TA00287A

eluting from the column gradually increases, thus conforming a breakthrough curve. The recorded signal during this process of continuous circulation of the adsorbate through the column is called a frontal or primary chromatogram. The concept of a frontal chromatogram is to obtain this effluent frontal chromatogram, the concentration of which is measured at the exit of the column, using standard analytical techniques. At the initial stage, pure solvent exits throughout the adsorbent column as the sorbate molecules are becoming adsorbed on to the adsorbent. When the front has passed through the whole column (i.e., when the adsorbent is saturated), the concentration of the solution that comes out of the column suddenly increases and eventually reaches a plateau. The frontal chromatogram is typically characterized by a sigmoidal front and a plateau at the end as shown in Figure 14.[114] From the mean positions of the breakthrough curves, the concentration of the solute in the feed solution and the mass of the adsorbent in the column, it is possible to extract information about the characteristic properties of the adsorbents such as the number of adsorption sites and the associated binding energies. This information can be obtained from the mean positions of the breakthrough curves as a function of initial concentration. The mean position of breakthrough curve gives characteristic information about the number of moles of the adsorbate required to saturate the adsorbent in the column and this varies depending on the initial concentration. Thus, information about the binding energy and the total adsorption capacity can be obtained by measuring the mean breakthrough time for different initial adsorbate concentration and plotting them according to the previously described Langmuir or other heterogeneous adsorption isotherms that relate q versus C_o; in FAC experiments C_o is equivalent to C_e at saturation.

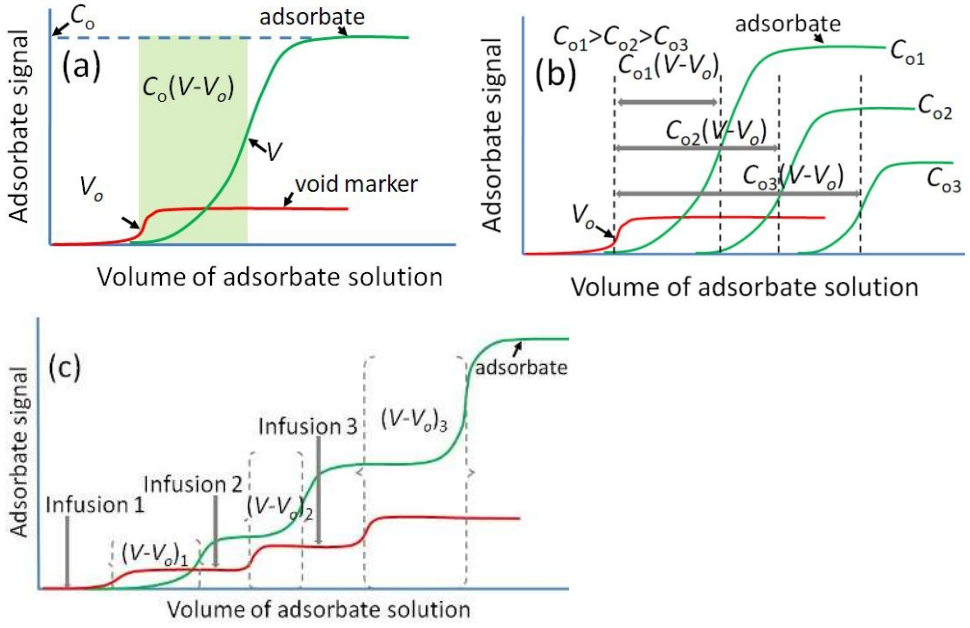

Figure 14: (a) A typical frontal chromatogram or breakthrough curve of the adsorbate from its solution of concentration C_o and a void marker; V_o represents breakthrough volume of the adsorbent in the absence of the binding event; V represents the breakthrough volume of the adsorbent during to the adsorption; (b) frontal chromatograms of the adsorbate (green) from its solution of different concentration, C_{o1}, C_{o2} and C_{o3}; also shown are the frontal chromatogram of

View Article Online
DOI: 10.1039/C9TA00287A

void marker which is infused with the adsorbate to obtain V_o (c) frontal chromatograms obtained using a 'modified staircase' experiment to obtain adsorption isotherms; the adsorbate(green) is infused at increasing concentrations from a initial concentration reaching to a final concentration along with a void marker (red).

The volume of solution that has passed through the column before the adsorbate breakthrough is called the retention volume. This volume includes a small volume of solution necessary to replace the solvent between the adsorbate particles in the column at the beginning of the experiments and this small volume is subtracted from the retention volume to obtain a corrected retention volume, $(V\text{-}V_o)$. The specific retention volume or the adsorption capacity of the adsorbent in the column can be obtained by dividing the retention volume by the mass of the adsorbent in the column (see Figure 14 a for more details). For a single-component adsorption, the amount of adsorbate filtered in the column can be obtained from a simple mass balance equation:

$$q = (V\text{-}V_o).C_o \quad (60)$$

where, C_o is the concentration of the adsorbate in the solution.

The above relation is usually expressed in terms of amount adsorbed per unit mass of adsorbent. The amount adsorbed can be plotted against the concentration, and the corresponding adsorption isotherm $f(C_o)$ can be obtained, as the amount adsorbed q refers to the mass of solute adsorbed which is in equilibrium with the solution concentration, C_o. The amount adsorbed can be written as:

$$q = f(C_o) = (\text{V-V}_o).C_o \quad (61)$$

Most of the liquid phase adsorption equilibrium data follow a Type 1 isotherm (IUPAC reference), the specific retention volume decreases with increase in concentration.

$$(V\text{-}V_o) = f(C_o)/C_o \quad (62)$$

When C_o tends to zero, the $(V\text{-}V_o)$ can reach a constant value equal to the slope (or Henry's isotherm constant) of the first linear part of the isotherm.

The adsorption equilibrium data for different adsorbate concentrations can be determined experimentally by obtaining the frontal chromatogram with adsorbate solution of initial concentration as shown in Figure 14b. Alternatively, a modified staircase approach can be used in which the adsorbate solution of different initial concentration is introduced in to the column sequentially without any washing steps in between, starting with the lowest of a series of initial concentration(the concept is shown in Figure 14c). The specific retention volume is determined for each of the adsorbate concentration in the solution and this way the binding parameters can be determined from a single experiment. In the modified stair-case approach the initial concentration refers to the concentration of adsorbate in solution for the first step, whereas for

View Article Online
DOI: 10.1039/C9TA00287A

the second step (or second infusion as shown in Figure 14c) it is the sum of the initial concentration of the solute in the first step plus the adsorbate concentration in the second step. Likewise, for the case of third step, the concentration is the sum of the adsorbate concentration in the first, second and third step and so on for the remaining steps. Similar to the conventional frontal analysis experiments, the retention volume is obtained by monitoring both the retention volume and the solution volume required to replace the solvent between the adsorbent particles in the adsorbent column. V_o can be measured by continuously including a compound in the adsorbate solution that can act like a void marker. This void marker should have no affinity to the adsorbent. The stair-case experiments can be performed over a wide range of initial concentrations of interest. Alternatively, all the active sites on the adsorbents can be titrated by simultaneously increasing the sorbate concentration in the solution until the specific retention volume of the adsorbent reaches to a minimum.

In Figure 15a we show the adsorption isotherm of component A from its single and binary mixture. The data can be fitted to a theoretical isotherm to determine the binding site energy distribution by using any one of the methods discussed above. Figure 15b shows the corresponding site energy distribution obtained using the finite difference method (discussed in section 8) based on a Langmuir-Freundlich isotherm (the constants are shown in Figure 15a). Adsorption of component A from a binary fluid mixture exhibits a more homogeneous (quasi-Gaussian) distribution of binding site energies. The adsorption from single component shows a heterogeneous distribution of binding site energies. One noteworthy interpretation of Figure 15b is that the presence of a secondary component in the fluid mixtures decreases the sites with highest binding energy. In this way, it is possible to determine the change in the distribution of site energies due to the competition effects. FAC can be a versatile and complementary technique to the above discussed methods that can predict the binding site energy distribution.

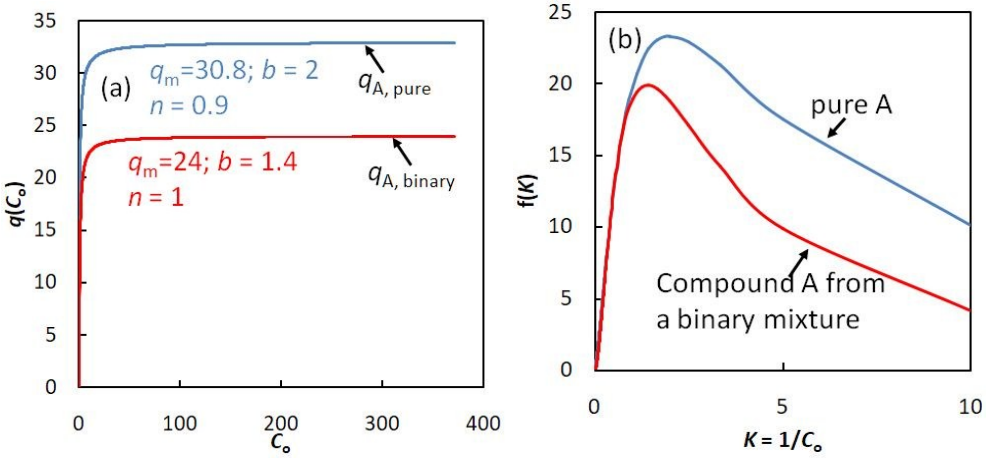

Figure 15: (a) Adsorption isotherm of component A from its pure solution ($q_{A,pure}$) and from a binary mixture ($q_{A,binary}$) that contains another component in addition to A (also shown are the Langmuir-Freundlich isotherm constants); (b) site energy distribution spectra for adsorption (site energy distribution function was obtained using the finite different method – see section 8).

View Article Online
DOI: 10.1039/C9TA00287A

13. Adsorption calorimetry

Calorimetry is extensively used to characterize the surface heterogeneity by measuring the heat exchanges involved during the physical (or chemical) adsorption process. The site energy distribution is defined in terms of the adsorption heat involved rather than the frequency distribution or any other similar mathematical function. The experimental details of this technique is beyond the scope of this review and has been covered in detail in the classic work of Roquerol et al [115] and in the lecture report of Christensen[116]. Rather, the principles of adsorption calorimetry are briefly covered in the context of this review.

Calorimetry can detect the specific interactions between adsorbent and adsorbate and can detect phase changes occurring in the adsorbed layer and in some cases can even detect any change involved in the extent of the solid-fluid interface. The heat involved in physisorption is usually small and requires high sensitivity and stability. Calorimetry exists in several variants: adiabatic, isothermal and heat-flow calorimeters. Heat-flow calorimeters possess the high stability required for interfacial calorimetry as this technique uses thermocouples (ensuring thermal conduction between the calorimetric cell and its surrounding) to measure the heat flow. Calorimetric experiments are often performed to measure integral heat or the differential heat of adsorption. These values can be obtained depending on the mode of the operation. In Figure 15 two modes are shown, either closed or open mode while measuring the adsorption heat. In closed mode (Figure 16 a), the volume of B is negligible, and the volume of C equals the volume of the adsorbent and thus the total volume remains constant and there is no volume work. If the pure and dry solid (placed in C) is placed in contact with a wetted or pure liquid (placed in A), then the adsorbed heat should be equal to the heat of immersion. In open mode, the adsorption is usually increased in small steps and the corresponding heat change in C is measured. Based on the working principles, the first one (closed mode) is often referred to as immersion calorimetry or wetting calorimetry and latter one is referred to as adsorption calorimetry (this set-up allows for measurement of the differential heat).[115,117,118] An adsorbent might contain a wide range of binding sites and if all the sites are titrated with the guest molecule, the evolved heat will be an integral heat. In this case, if we know the number of adsorbed molecules, then the mean heat of adsorption can be calculated. The heat value obtained in this manner is sensitive to the state of the solid surface. The heat will vary if the solid adsorbents are fully evacuated or if there is already any pre-adsorbed gases on the surface or within the pore volume. For the case of completely evacuated solids, the integral heat (also called heat of immersion) is numerically equal to the difference between the integral heat of adsorption at saturation pressure and the heat of vaporization of the liquid. As the guest molecules are provided in excess to that of the number of available sites on the adsorbent surface, measuring the adsorption this way will lead to loss of information about the number of molecules adsorbed on to the known amount of solid. Based on the working principles, the q_{imm} is simply equal to the negative value of the heat of immersion (ΔH_{imm}) or the heat of wetting (ΔH_{wett}). These enthalpy changes are defined (at constant temperature) as the difference between the transitions from a starting point, which is the energy of the solid, to the establishment of a solid-liquid interface.

In the case of differential heats of adsorption, the adsorption sites with different binding energies will be titrated progressively and the associated energies can be determined. As in the open mode

View Article Online
DOI: 10.1039/C9TA00287A

(Figure 16(b)), via moving the piston down, the adsorption can be increased in small steps and the heat evolved in C only will be measured to obtain the adsorption heat. The set-up shown in Figure 16(b) is an oversimplified version of a typical adsorption microcalorimeter which is usually connected to a volumetric apparatus that allows determination of the adsorbed doses and the equilibrium pressure; a detailed instrumental set-up can be found elsewhere.[119,120] In this case, the heat evolved is attributed to a definite amount of adsorbed molecules but on an unknown amount of surface.[121] On the other hand this is a doubly quantitative technique as it allows for determination of both the amounts adsorbed and the evolved heats. The adsorption heat measured here corresponds to the difference between the energies involved during the transition from a starting point, which is the energy of a dry or a partly wet solid, to establishment of a new solid-liquid interface. In principle, the heat evolved can be obtained as a function of the moles adsorbed; this means the adsorption sites can be progressively titrated with a suitable probe (adsorbate) molecule and its corresponding binding energy can be estimated.

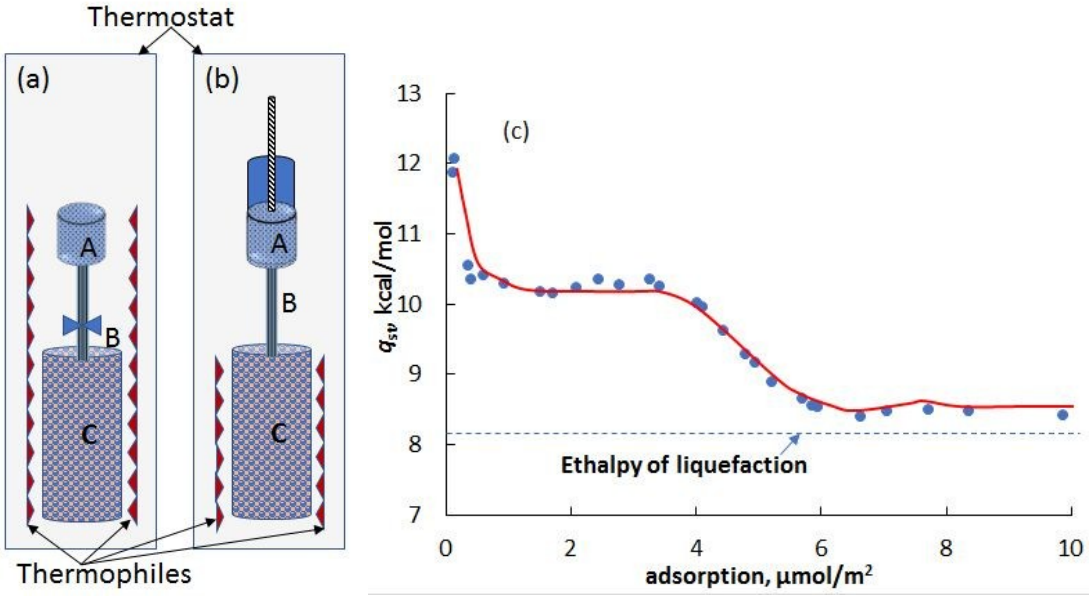

Figure 16: Two different operational modes of adsorption calorimetry (a) closed mode, where liquid is placed in cell and the adsorbent is in C. A and B are connected via a small tube of negligible volume; opening B will allow the adsorbent to immerse completely in the liquid; the heat evolved in the total system (A+B+C) is measured (b) open mode, where the adsorbent in C is connected to the gas cell in A; by moving the piston down the adsorption loading can be increased in small steps and here the heat evolved in part C is measured; Figure 16(a and b) was redrawn based on the images shown in the work of Lyklema et al., [122] (c) The differential heat of adsorption of benzene vapor at 20 ^{o}C as a function of surface coverage of a graphitized thermal black; the data was measured by Isirikyan and Kiselev.[123]

Traditionally, adsorption calorimetry is used to characterize catalyst materials and in the area of adsorption mostly to characterize zeolitic materials, a wide range of porous carbon based adsorbents and more recently to characterize metal organic frameworks.[120,122,124,125] Figure 16(c)

View Article Online
DOI: 10.1039/C9TA00287A

shows the differential heat measured by adsorption of non-polar fluid benzene on to graphitized thermal blacks at 20 °C as experimentally measured by Isirikyan and Kiselev.[123] As benzene is a neutral molecule, the differential heat obtained should practically correspond only to the dispersion forces or the Van der Waals interactions. The multiple regions in Figure 16(c) can be used provide multiple insights on the adsorption process and also on the type of the adsorption sites on the adsorbent surface. Theoretically, it is expected that the adsorption heat is a decreasing function of the amount adsorbed signifying the surface is energetically heterogeneous where the surface with highest binding energy will be filled first. However Figure 16(c) clearly shows an enhanced adsorption heat (11-12 kcal/mol) at lower coverage (n = 0.117-0.9 μmol/m^2). This was explained by the penetration of the benzene molecules into the grain boundaries of the single crystals of graphite. The heat of adsorption was almost constant and equal to 10.3 kcal/mole beginning from n = 0.325 to3.38 μmol/m^2, after which it falls sharply indicating the transition from monolayer to multilayer adsorption. The adsorption heat eventually drops close to the heat of condensation of benzene (~ 8.4 kcal/mol) during the formation of the second monolayer; the adsorption heat of second layer differs from the heat of condensation roughly by 0.5 kcal/mol. These results clearly indicate that there is presence of low concentration of high energetic binding sites due to the grain boundaries and possibly even due to line defects. The constant adsorption heat from n = 0.325 to 3.38 μmol/m^2 can be attributed to the perfect match between the benzene molecules and the graphite-like surface structure. The drop in isosteric heat associated with the adsorption from n = 3.38 to 5.9 μmol/m^2 confirms the presence of energetic heterogeneity created by the pre-adsorbed benzene molecules. Similar to that details in Figure 16(c), much information can be obtained using calorimetric techniques. Calorimetric techniques can be especially useful when adsorption involves strong chemisorption forces. Recently, Gassensmith *et al*.,[120] used adsorption calorimetry to expose the presence of adsorption sites in a model metal organic frameworks, CD-MOF-2 and hosts CO_2 molecule via both chemisorption and physisorption. An adsorption heat value of 27.12 kcal/mol for the chemisorption site and 15.63 kcal/mol at the adsorption sites where CO_2 is adsorbed only via physisorption, were obtained experimentally. Immersion calorimetry can also provide information that allows comparison of the binding affinity of the adsorbent surfaces for targeted molecules; the only difference being that ΔH_{imm} gives information about the whole energy evolved at a constant temperature. For instance, the heat of immersion of basic alumina in water and HCl can provide information about the basicity of the adsorbent surface and how strongly a suitable adsorbent can host HCl. [126]

It is essential to mention here that adsorption calorimetry is the best experimental technique to provide information that is obtained analytically using the site energy distribution spectra. The only difference is that for the case of the site energy distribution function, it is possible to get the frequency distribution of the adsorption site energies as a function of bulk pressure without having any information about the heat exchange involved. Additionally, site energy distribution spectra can be obtained directly from the existing adsorption isotherms without any requirement

View Article Online
DOI: 10.1039/C9TA00287A

for additional experimental set-up. In that spirit, both techniques can complement each other in predicting the energetic heterogeneity of the adsorbent surface. To date, little work has been reported comparing both techniques to characterize the surface properties of the adsorbents. It would be an interesting contribution to the field to perform such studies in order to investigate the complementarity of adsorption calorimetry and the mathematical approaches discussed in this review.

14. Final remarks

Determining the forces involved during the adsorption processes can garner many interesting information about the mechanism. This has conventionally been achieved by studying the adsorption equilibrium data based on theoretical adsorption isotherms or using chromatographic and calorimetric techniques. Alternatively, such information can be obtained directly from either discrete or continuous site energy distribution spectra. The techniques described are relatively simple to implement and can obtain the site energy distribution spectra of the adsorbents without the requirement of any complex mathematics or sophisticated coding. Emphasis is placed on the importance of the adsorption equilibrium data or the theoretical isotherms and how these data can be exploited to obtain additional information about the adsorption site heterogeneity. The methods discussed here have a common assumption which is the heterogeneity of the adsorbent surfaces are characterized by the presence of several homottatic patches that can be modeled using the generalized adsorption integral expression. This simple assumption is enough to model most of the adsorbents that are encountered in laboratory or industrial adsorbents. It should be stressed that, irrespective of the methods discussed here, the site energy distribution spectra will depend on the type of theoretical adsorption isotherms used. So, it is the choice of the user to determine the site energy distribution based on a specific theoretical isotherm.

This is not a challenging task as many theoretical isotherms are available to fit the experimental adsorption equilibrium data using simple linear or non-linear regression analysis. Once the best-fit isotherm is found, any of the methods discussed above can be used to determine the adsorption site energy distribution spectra. To date, adsorption isotherms are seldom used to determine the isotherm capacity. In the case of new materials, adsorption isotherms are used to find the material properties like surface area and pore volume. This review has showed the isotherms can be further exploited to give additional material properties, like how many different types of adsorption sites, their adsorption energies, how they are distributed on the surface, selectivity for hosting a target molecule, and how sensitive the adsorption is to the temperature effects, etc. Clearly, such information is highly valuable in the area of gas storage, gas separation, wastewater treatment and also can serve as a new way to compare the fundamental performance of porous materials for a specific target application. To date, comparison of material properties is based on the sorption potential. Alternatively, they can be compared in terms of their mean binding energy, how the adsorption site energies are distributed, either narrow or broad quasi-Gaussian distribution, etc. This can serve as a reliable approach in the area of material characterization. For instance, in the area of natural gas storage or hydrogen storage, it is possible to compare what type of materials exhibit a higher deliverable capacity, higher storage capacity

View Article Online
DOI: 10.1039/C9TA00287A

and how the adsorption site energies are distributed in those materials. This comparison can be made under different experimental conditions, such as at cryogenic or room temperature. In the case of H_2 storage, it is essential to understand the forces involved during the storage of this important molecule at both conditions.

Practically, the Clausius-Clapeyron equation is not applicable when the adsorption isotherms are obtained at two different temperatures that differ by more than 5 to 10 ^{o}C. Affinity distribution spectra can fill this gap and provide a reliable and comparable picture about the forces involved. This technique can also be exploited in the area of materials design or to expose the effect of post-treatment like surface functionalization on the distribution of site energies. Provided we have a high-resolution adsorption isotherm, we can obtain information about what type of adsorption sites are more emphasized after post-treatment for a specific target molecule. The methods discussed above are simple, fast (obtained within minutes) and do not require any specialized equipment.

Material development is a key research area in the field of gas storage, gas separation, wastewater treatment, drug discovery, chromatography, wastewater treatment, etc. Every day, new materials are being discovered. Information about the surface properties of these materials will provide the essential information required for screening of these materials for targeted applications or at least to allow comparison of the performance of different types and classes of materials for a specific application. In that spirit, this review will serve as a useful guide for the characterization of materials for their adsorption and general active site properties.

Acknowledgment
We thank EU for the Intra European Marie Curie Research Fellowship (PIEF-GA-2013-623227).
Thanks to Laura Gonzalez Saladich for the cover art design.

View Article Online
DOI: 10.1039/C9TA00287A

References

1 J. Feher and J. Feher, *Quant. Hum. Physiol.*, 2017, 853–869.
2 T. K. Dam and C. F. Brewer, *Methods Enzymol.*, 2003, **362**, 455–486.
3 S. Gadipelli, H. A. Patel and Z. Guo, *Adv. Mater.*, 2015, **27**, 4903–4909.
4 S. Gadipelli, W. Travis, W. Zhou and Z. Guo, *Energy Environ. Sci.*, 2014, **7**, 2232–2238.
5 G. Srinivas, J. Burress and T. Yildirim, *Energy Environ. Sci.*, 2012, **5**, 6453.
6 S. Gadipelli, Y. Lu, N. T. Skipper, T. Yildirim and Z. Guo, *J. Mater. Chem. A*, 2017, **5**, 17833–17840.
7 G. Srinivas, V. Krungleviciute, Z.-X. Guo and T. Yildirim, *Energy Environ. Sci.*, 2014, **7**, 335–342.
8 S. Gadipelli, H. A. Patel and Z. Guo, *Adv. Mater.*, 2015, **27**, 4903–4909.
9 K. V. Kumar, K. Preuss, L. Lu, Z. X. Guo and M. M. Titirici, *J. Phys. Chem. C*, 2015, **119**, 22310–22321.
10 R. Khosravi, A. Azizi, R. Ghaedrahmati, V. K. Gupta and S. Agarwal, *J. Ind. Eng. Chem.*, 2017, **54**, 464–471.
11 S. Gadipelli and Z. Guo, *Chem. Mater.*, 2014, **26**, 6333–6338.
12 S. Gadipelli and Z. X. Guo, *ChemSusChem*, 2015, **8**, 2123–2132.
13 G. Srinivas and Z. X. Guo, *Prog. Mater. Sci.*, 2014, **69**, 1–60.
14 S. Shinohara, Y. Chiyomaru, F. Sassa, C. Liu, K. Hayashi, S. Shinohara, Y. Chiyomaru, F. Sassa, C. Liu and K. Hayashi, *Sensors*, 2016, **16**, 1974.
15 N. B. McKeown and P. M. Budd, *Chem. Soc. Rev.*, 2006, **35**, 675.
16 S. Cavenati, C. A. Grande and A. E. Rodrigues, *Chem. Eng. Sci.*, 2006, **61**, 3893–3906.
17 V. K. Gupta, P. J. M. Carrott, M. M. L. Ribeiro Carrott and Suhas, *Crit. Rev. Environ. Sci. Technol.*, 2009, **39**, 783–842.
18 I. Ali and V. K. Gupta, *Nat. Protoc.*, 2007, **1**, 2661–2667.
19 K. V. Kumar, K. Preuss, M.-M. Titirici and F. Rodríguez-Reinoso, *Chem. Rev.*, 2017, **117**, 1796–1825.
20 K. V. Kumar, E. A. Müller and F. Rodríguez-Reinoso, *J. Phys. Chem. C*, 2012, **116**, 11820–11829.
21 K. V. Kumar, K. Preuss, Z. X. Guo and M. M. Titirici, *J. Phys. Chem. C*, 2016, **120**, 18167–18179.
22 X. Pang and H.-X. Zhou, *Annu. Rev. Biophys.*, 2017, **46**, 105–130.
23 K. V. Kumar, M. C. Monteiro de Castro, M. Martinez-Escandell, M. Molina-Sabio and F. Rodriguez-Reinoso, *ChemPhysChem*, 2010, **11**, 2555–2560.
24 M. Molina-Sabio, M. T. Gonzalez, F. Rodriguez-Reinoso and A. Sepúlveda-Escribano, *Carbon N. Y.*, 1996, **34**, 505–509.
25 M. Thommes, K. Kaneko, A. V Neimark, J. P. Olivier, F. Rodriguez-Reinoso, J. Rouquerol and K. S. W. Sing, *Pure Appl. Chem*, 2015, aop.
26 W. Rudzinski and D. H. (Douglas H. Everett, *Adsorption of gases on heterogeneous surfaces*, Academic Press, 1992.
27 K. V. Kumar, M. Monteiro de Castro, M. Martinez-Escandell, M. Molina-Sabio and F. Rodriguez-Reinoso, *Phys. Chem. Chem. Phys.*, 2011, **13**, 5753.
28 W. Rudziński, M. Jaroniec, S. Sokolowski and G. F. Cerofolini, *Czechoslov. J. Phys.*, 1975, **25**, 891–901.
29 K. V. Kumar, A. M. Silvestre-Albero and F. Rodriguez-Reinoso, *RSC Adv.*, 2012, **2**, 784–788.
30 H. G. Weder, J. Schildknecet, R. A. Lutz and P. Kesselrinu, *Determination of Binding Parameters from Scatchard Plots Theoretical and Practical Considerations*, 1974, vol. 42.
31 K. V. Kumar, M. M. de Castro, M. Martinez-Escandell, M. Molina-Sabio and F. Rodriguez-

View Article Online
DOI: 10.1039/C9TA00287A

Reinoso, *J. Phys. Chem. C*, 2010, **114**, 13759–13765.
32 H. Freundlich and W. Heller, *J. Am. Chem. Soc.*, 1939, **61**, 2228–2230.
33 O. Redlich and D. L. Peterson, *J. Phys. Chem.*, 1959, **63**, 1024–1024.
34 R. Sips, *J. Chem. Phys.*, 1950, **18**, 1024–1026.
35 R. Sips, *J. Chem. Phys.*, 1948, **16**, 490–495.
36 L. Ortiz, *Masters Sci. Thesis, Univ. Missouri-Columbia*.
37 K. Mosher, J. He, Y. Liu, E. Rupp and J. Wilcox, *Int. J. Coal Geol.*, 2013, **109–110**, 36–44.
38 I. Langmuir, *J. Am. Chem. Soc.*, 1918, **40**, 1361–1403.
39 I. M. Klotz and D. L. Hunston, *Biochemistry*, 1971, **10**, 3065–3069.
40 D. G. Kinniburgh, *Environ. Sci. Technol.*, 1986, **20**, 895–904.
41 K. V. Kumar, K. Porkodi and F. Rocha, *J. Hazard. Mater.*, 2008, **151**, 794–804.
42 K. V. Kumar and S. Sivanesan, *J. Hazard. Mater.*, 2005, **123**, 288–292.
43 K. V. Kumar and S. Sivanesan, *J. Hazard. Mater.*, 2005, **126**, 198–201.
44 K. Porkodi and K. Vasanth Kumar, *J. Hazard. Mater.*, 2007, **143**, 311–327.
45 K. Vasanth Kumar and S. Sivanesan, *J. Hazard. Mater.*, 2006, **134**, 237–244.
46 K. V. Kumar, V. Ramamurthi and S. Sivanesan, *J. Colloid Interface Sci.*, 2005, **284**, 14–21.
47 G. Scatchard, *Ann. N. Y. Acad. Sci.*, 1949, **51**, 660–672.
48 L. Susskind and A. Friedman, *Quantum mechanics : the theoretical minimum*, Penguin, 2015.
49 J. P. Olivier and S. Ross, *Proc. R. Soc. London. Ser. A. Math. Phys. Sci.*, 1962, **265**, 447–454.
50 S. Ross, in *Fundamental Phenomena in the Materials Sciences*, Springer US, Boston, MA, 1966, pp. 109–137.
51 W. Rudzinski and D. H. (Douglas H. Everett, *Adsorption of gases on heterogeneous surfaces*, Academic Press, 1992.
52 K. V. Kumar, S. Gadipelli, K. Preuss, H. Porwal, T. Zhao, Z. X. Guo and M.-M. Titirici, *ChemSusChem*, 2017, **10**, 199–209.
53 C. Sanford and S. Ross, *J. Phys. Chem.*, 1954, **58**, 288–288.
54 A. K. Singh, J. Lu, R. S. Aga and B. I. Yakobson, *J. Phys. Chem. C*, 2011, **115**, 2476–2482.
55 K. V. Kumar, A. Salih, L. Lu, E. A. Müller and F. Rodríguez-Reinoso, *Adsorpt. Sci. Technol.*, 2011, **29**, 799–817.
56 G. K. Dimitrakakis, E. Tylianakis and G. E. Froudakis, *Nano Lett.*, 2008, **8**, 3166–3170.
57 K. Gubbins, Storing Natural Gas, https://www.psc.edu/science/Gubbins/Gubbins-gas.html, (accessed 30 November 2018).
58 G. F. Cerofolini, *Surf. Sci.*, 1975, **47**, 469–476.
59 G. F. Cerofolini, *Chem. Phys.*, 1978, **33**, 423–434.
60 M. C. Carter, J. E. Kilduff and W. J. Weber, *Site Energy Distribution Analysis of Rreloaded Adsorbents*, 1995, vol. 29.
61 M. C. Carter, J. E. Kilduff and W. J. Weber, *Site Energy Distribution Analysis of Rreloaded Adsorbents*, 1995, vol. 29.
62 K. V. Kumar, J. C. Serrano-Ruiz, H. K. S. Souza, A. M. Silvestre-Albero and V. K. Gupta, *J. Chem. Eng. Data*, 2011, **56**, 2218–2224.
63 T. L. Hill, *J. Chem. Phys.*, 1949, **17**, 762–771.
64 D. L. Hunston, *Anal. Biochem.*, 1975, **63**, 99–109.
65 D. L. Hunston, *Anal. Biochem.*, 1975, **63**, 99–109.
66 K. Ninomiya and J. D. Ferry, *J. Colloid Sci.*, 1963, **18**, 421–432.
67 A. K. Thakur, P. J. Munson, D. L. Hunston and D. Rodbard, *Anal. Biochem.*, 1980, **103**, 240–254.
68 R. J. Umpleby, S. C. Baxter, M. Bode, J. K. Berch, R. N. Shah and K. D. Shimizu, *Anal. Chim.*

View Article Online
DOI: 10.1039/C9TA00287A

Acta, 2001, **435**, 35–42.
69 Ravichandar Babarao, and Zhongqiao Hu, J. Jiang*, S. Chempath and S. I. Sandler, , DOI:10.1021/LA062289P.
70 S. Gao, C. G. Morris, Z. Lu, Y. Yan, H. G. W. Godfrey, C. Murray, C. C. Tang, K. M. Thomas, S. Yang and M. Schröder, *Chem. Mater.*, 2016, **28**, 2331–2340.
71 B. Liu, S. Yao, X. Liu, X. Li, R. Krishna, G. Li, Q. Huo and Y. Liu, *ACS Appl. Mater. Interfaces*, 2017, **9**, 32820–32828.
72 B. J. Stanley and G. Guiochon, *Numerical Estimation of Adsorption Energy Distributions from Adsorption Isotherm Data with the Expectation-Maximization Method*, 1993, vol. 97.
73 B. J. Stanley, P. Szabelski, Y.-B. Chen, B. Sellergren and G. Guiochon*, , DOI:10.1021/LA020747Y.
74 Q. Li, X. Ning, Y. An, B. J. Stanley, Y. Liang, J. Wang, K. Zeng, F. Fei, T. Liu, H. Sun, J. Liu, X. Zhao and X. Zheng, *Anal. Chem.*, 2018, **90**, 7903–7911.
75 F. Gritti and G. Guiochon, *J. Chromatogr. A*, 2007, **1144**, 208–220.
76 B. J. Stanley and G. Guiochon, *Calculation of Adsorption Energy Distributions of Silica Samples Using Nonlinear Chromatography*, 1995, vol. 11.
77 K. V. Kumar, K. Preuss, M.-M. Titirici and F. Rodríguez-Reinoso, *Chem. Rev.*, 2017, **117**, 1796–1825.
78 F. Rodriguez-Reinoso, *Pure Appl. Chem.*, 1989, **61**, 1859–1866.
79 K. S. Bharathi and S. T. Ramesh, *Appl. Water Sci.*, 2013, **3**, 773–790.
80 A. J. Howarth, A. W. Peters, N. A. Vermeulen, T. C. Wang, J. T. Hupp and O. K. Farha, *Chem. Mater.*, 2017, **29**, 26–39.
81 Z.-G. Wang*, , DOI:10.1021/IE051136E.
82 V. Kamble and A. Umarji, *AIP Adv.*, 2015, **5**, 037138.
83 N. Z. Misak, *Colloids Surfaces A Physicochem. Eng. Asp.*, 1995, **97**, 129–140.
84 C. Baggiani, G. Giraudi, C. Giovannoli, C. Tozzi and L. Anfossi, *Anal. Chim. Acta*, 2004, **504**, 43–52.
85 † C. L. McCallum, ‡ T. J. Bandosz, † S. C. McGrother, § and E. A. Müller and ⊥ K. E. Gubbins*, , DOI:10.1021/LA9805950.
86 E. A. Müller, L. F. Rull, L. F. Vega and K. E. Gubbins, *J. Phys. Chem.*, 1996, **100**, 1189–1196.
87 A. Boutin, F.-X. Coudert, M.-A. Springuel-Huet, A. V. Neimark, G. Férey and A. H. Fuchs, *J. Phys. Chem. C*, 2010, **114**, 22237–22244.
88 M. Shivanna, Q.-Y. Yang, A. Bajpai, E. Patyk-Kazmierczak and M. J. Zaworotko, *Nat. Commun.*, 2018, **9**, 3080.
89 G. Srinivas, W. Travis, J. Ford, H. Wu, Z.-X. Guo and T. Yildirim, *J. Mater. Chem. A*, 2013, **1**, 4167.
90 T. Düren, Y.-S. Bae and R. Q. Snurr, *Chem. Soc. Rev.*, 2009, **38**, 1237.
91 L. G. Joyner and P. H. Emmett, *J. Am. Chem. Soc.*, 1948, **70**, 2359–2361.
92 S. Brunauer, *The Adsorption of Gases and Vapors Vol I - Physical Adsorption*, Oxford University Press, London, 1943.
93 E. . Swan and A. R. Urquhart, *J. Phys. Chem.*, 1927, **31**, 251–276.
94 S. Brunauer, *The adsorption of gases and vapors*, Princeton University Press, 1943.
95 D. G. Dobay, Y. Fu and F. E. Bartell, *J. Am. Chem. Soc.*, 1951, **73**, 308–314.
96 R. A. Beebe, J. Biscoe, W. R. Smith and C. B. Wendell, *J. Am. Chem. Soc.*, 1947, **69**, 95–101.
97 F. J. Wilkins, *Proc. R. Soc. A Math. Phys. Eng. Sci.*, 1938, **164**, 496–509.
98 L. G. Joyner and P. H. Emmett, *J. Am. Chem. Soc.*, 1948, **70**, 2353–2359.

View Article Online
DOI: 10.1039/C9TA00287A

99 R. A. Beebe, J. Biscoe, W. R. Smith and C. B. Wendell, *J. Am. Chem. Soc.*, 1947, **69**, 95–101.
100 L. G. Joyner and P. H. Emmett, *J. Am. Chem. Soc.*, 1948, **70**, 2353–2359.
101 A. Gotzias, E. Tylianakis, G. Froudakis and T. Steriotis, *Microporous Mesoporous Mater.*, 2015, **209**, 141–149.
102 L. Czepirski and J. JagiełŁo, *Chem. Eng. Sci.*, 1989, **44**, 797–801.
103 R. M. Barrer and J. A. Davies, *Proc. R. Soc. A Math. Phys. Eng. Sci.*, 1970, **320**, 289–308.
104 R. M. Barrer and A. G. Kanellopoulos, *J. Chem. Soc. A Inorganic, Phys. Theor.*, 1970, **0**, 765.
105 R. S. Bradley, *London, Edinburgh, Dublin Philos. Mag. J. Sci.*, 1931, **11**, 690–696.
106 A. G. Bezus, A. V. Kiselev, Z. Sedlaček and P. Q. Du, *Trans. Faraday Soc.*, 1971, **67**, 468–482.
107 L. Lu, S. Wang, E. A. Müller, W. Cao, Y. Zhu, X. Lu and G. Jackson, *Fluid Phase Equilib.*, 2014, **362**, 227–234.
108 K. Vasanth Kumar and F. Rodríguez-Reinoso, *RSC Adv.*, 2012, **2**, 9671.
109 S. A. Busev, S. I. Zverev, O. G. Larionov and E. S. Jakubov, *J. Chromatogr. A*, 1982, **241**, 287–294.
110 O. Lisec, P. Hugo and A. Seidel-Morgenstern, *J. Chromatogr. A*, 2001, **908**, 19–34.
111 Y. A. Eltekov, Y. V. Kazakevich, A. V. Kiselev and A. A. Zhuchkov, *Chromatographia*, 1985, **20**, 525–528.
112 S. Claesson, *Ann. N. Y. Acad. Sci.*, 1948, **49**, 183–203.
113 A. Tiselius, *Adv. Protein Chem.*, 1947, **3**, 67–93.
114 Y. A. Eltekov, Y. V. Kazakevich, A. V. Kiselev and A. A. Zhuchkov, *Chromatographia*, 1985, **20**, 525–528.
115 F. Rouquerol, J. (Jean) Rouquerol and K. S. W. Sing, *Adsorption by powders and porous solids : principles, methodology, and applications*, Academic Press, 1999.
116 J. J. Christensen, in *Thermochemistry and Its Applications to Chemical and Biochemical Systems*, Springer Netherlands, Dordrecht, 1984, pp. 1–16.
117 F. Rodríguez-Reinoso, A. M. Molina-Sabio and M. T. González, *Langmuir*, 1997, **13**, 2354–2358.
118 P. C. Gravelle, *Catal. Rev.*, 1977, **16**, 37–110.
119 B. Fubini, *Thermochim. Acta*, 1988, **135**, 19–29.
120 D. Wu, J. J. Gassensmith, D. Gouvêa, S. Ushakov, J. F. Stoddart and A. Navrotsky, *J. Am. Chem. Soc.*, 2013, **135**, 6790–6793.
121 J. M. DOUILLARD and F. SALLES, 2004, pp. 118–152.
122 J. Lyklema, H. P. van Leeuwen, T. van Vliet, A. M. (Anne-M. Cazabat, A. de Keizer, B. H. Bijsterbosch, G. J. (Gerard J. . Fleer and M. A. Cohen Stuart, *Fundamentals of interface and colloid science*, .
123 A. A. Isirikyan and A. V. Kiselev, *J. Phys. Chem.*, 1961, **65**, 601–607.
124 P. Le Parlouër, 2013, pp. 51–101.
125 J. Vernimmen, M. Guidotti, J. Silvestre-Albero, E. O. Jardim, M. Mertens, O. I. Lebedev, G. Van Tendeloo, R. Psaro, F. Rodríguez-Reinoso, V. Meynen and P. Cool, *Langmuir*, 2011, **27**, 3618–3625.
126 R. . Bailey and J. . Wightman, *J. Colloid Interface Sci.*, 1979, **70**, 112–123.